

Systematic evaluation of biofilm models for engineering practice: components and critical assumptions

J. P. Boltz, E. Morgenroth, D. Brockmann, C. Bott, W. J. Gellner and P. A. Vanrolleghem

ABSTRACT

Biofilm models are valuable tools for the design and evaluation of biofilm-based processes despite several uncertainties including the dynamics and rate of biofilm detachment, concentration gradients external to the biofilm surface, and undefined biofilm reactor model calibration protocol. The present investigation serves to (1) systematically evaluate critical biofilm model assumptions and components and (2) conduct a sensitivity analysis with the aim of identifying parameter subsets for biofilm reactor model calibration. AQUASIM was used to describe submerged-completely mixed combined carbon oxidation and nitrification IFAS and MBBR systems, and tertiary nitrification and denitrification MBBRs. The influence of uncertainties in model parameters on relevant model outputs was determined for simulated scenarios by means of a local sensitivity analysis. To obtain reasonable simulation results for partially penetrated biofilms that accumulated a substantial thickness in the modelled biofilm reactor (e.g. 1,000 μm), an appropriate biofilm discretization was applied to properly model soluble substrate concentration gradients and, consistent with the assumed mechanism for describing biofilm biomass distribution, biofilm biomass spatial variability. The MTBL thickness had a significant impact on model results for each of the modelled reactor configurations. Further research is needed to develop a mathematical description (empirical or otherwise) of the MTBL thickness that is relevant to modern biofilm reactors. No simple recommendations for a generally applicable calibration protocol are provided, but sensitivity analysis has been proven to be a powerful tool for the identification of highly sensitive parameter subsets for biofilm (reactor) model calibration.

Key words | AQUASIM, biofilm, calibration, design, identifiability, model, nitrogen removal, parameter, wastewater

INTRODUCTION

A mathematical biofilm model has been included in a majority of available wastewater treatment plant simulators that are used by practising engineers who seek to plan, evaluate, optimize, and/or design biofilm-based wastewater treatment processes. Practice based biofilm reactor modelling approaches typically use a one-dimensional (1-D) representation of the biofilm (see [Wanner *et al.* \(2006\)](#) for details). While there is agreement that a 1-D biofilm model is suitable (for most applications) when describing biofilm reactor performance, there are different modelling approaches

that require consideration (e.g. attachment/detachment, homogeneous vs. heterogeneous biomass distribution within the biofilm, mass transfer resistance external to the biofilm, and diffusivity within the biofilm).

Modelling approaches requiring consideration

The lack of a generally accepted systematic calibration protocol for biofilm reactor models leads to uncertainty among model users about how to best estimate model parameters

J. P. Boltz (corresponding author)
CH2M HILL, Inc.,
4350 W. Cypress Street, Suite 600,
Tampa, FL 33607,
USA
E-mail: jboltz@ch2m.com

E. Morgenroth
ETH Zürich,
Institute of Environmental Engineering,
8093 Zürich,
Switzerland

and

Eawag, Swiss Federal Institute of Aquatic Science
and Technology,
8600 Dübendorf,
Switzerland

D. Brockmann
INRA, UR0050,
Laboratoire de Biotechnologie de l'Environnement,
Avenue des Etangs,
Narbonne, F-11100,
France

C. Bott
Hampton Roads Sanitation District,
1440 Air Rail, Ave.,
Virginia Beach, VA 23455,
USA

W. J. Gellner
Hazen and Sawyer,
11311 Cornell Park Dr.,
Cincinnati, OH 45242,
USA

P. A. Vanrolleghem
Canada Research Chair in Water Quality Modelling,
modelEAU,
Université Laval, Pavillon Pouliot,
Québec (QC),
Canada G1K 7P4

and calibrate biofilm models. Both aspects are discussed in more detail below.

Attachment and detachment processes: The rate at which particles attach and detach from a biofilm has a marked impact on modelling results. In a modelling study, [Morgenroth & Wilderer \(2000\)](#) demonstrated that overall reactor performance and biofilm structure are significantly influenced by the mode of detachment. However, both biofilm attachment and detachment process mechanics are poorly understood; therefore, approaches to modelling these processes may have limited reliability and robustness when describing a biofilm reactor. Most heterogeneous 1-D biofilm models used in engineering practice (see [Boltz *et al.* \(2010b\)](#) for a comprehensive list) describe the rate of particle attachment (r_{at}) as a first-order process that is dependent on an attachment rate coefficient (k_{at}), bulk-liquid particle concentration (X_i), and biofilm area (A_F). Given the current state of science, experimental data is required to evaluate existing models, and develop and validate improved mathematical relationships describing the fate of particulate matter in biofilm reactors.

Steady-state biofilm models assume a constant biofilm thickness (L_F) and are applied under the premise that biofilm growth is balanced by a combination of internal loss (e.g. decay and hydrolysis, or endogenous respiration) and detachment. Consequently, detachment may not be modelled explicitly. However, the dynamic simulation of biofilms (and biofilm reactors) requires the inclusion of an explicit detachment model despite rather limited mechanistic understanding. Some rate expressions have been summarized by [Morgenroth & Wilderer \(2000\)](#) and [Morgenroth \(2003\)](#). Rate expressions applied to practice-oriented models have been summarized by [Boltz *et al.* \(2010b\)](#). The rate and category (i.e. abrasion, erosion, sloughing, and predator grazing) of detachment can have a significant influence on biofilm structure and, therefore, reactor simulation and performance ([Morgenroth 2003](#)). [Kissel *et al.* \(1984\)](#) stated that problems inherent to biofilm detachment modelling include a poor understanding of fundamental (biofilm detachment) process mechanics and the inability to predict exactly at what location inside the biofilm that detachment will occur. Biofilm detachment location is important when taking into account the distribution of a heterogeneous biofilm throughout a reactor either by combining multiple 1-D simulations or by 2-D or 3-D modelling ([Morgenroth *et al.* 2000](#)).

Biofilm structure: Mixed-culture biofilms that develop in combined carbon oxidation and nitrification biofilm reactors may be generally characterized by the spatial distribution of microorganisms throughout the biofilm. This spatial distribution is referred to as the biofilm structure

for the remainder of this paper. In these biofilms the faster growing heterotrophic bacteria tend to exist predominantly in biofilm locations near the bulk-liquid and biofilm interface. These heterotrophic bacteria overgrow autotrophic nitrifiers and establish a stratified biofilm (perpendicular to the growth medium) in which the nitrifiers exist deeper inside the biofilm ([Zhang *et al.* 1994](#); [Okabe *et al.* 1995](#)). As a result, heterotrophic bacteria have more direct access to substrates and macronutrients diffusing from the bulk liquid into the biofilm, but the bacteria are also more susceptible to detachment from the biofilm surface. The experimentally observed spatial distribution of heterotrophic and autotrophic bacteria in a mixed-culture biofilm growing in a combined carbon oxidation and nitrification biofilm reactor has been described by mathematical models of biofilms ([Kissel *et al.* 1984](#); [Wanner & Gujer 1984](#); [Rittmann & Manem 1992](#)). In heterogeneous 1-D biofilm models the observed spatial distribution of bacteria is described as a series of layers, which also describes the spatial distribution of soluble substrates. A homogeneous biofilm biomass distribution reduces the competitive advantage of heterotrophic bacteria that exists in a heterogeneous (layered) 1-D biofilm model, as heterotrophic and autotrophic bacteria are evenly distributed throughout the biofilm and have direct access to both substrates and macronutrients diffusing from the bulk liquid into the biofilm. A homogeneous biofilm biomass distribution can be modelled by introducing an artificial diffusion of all particulate compounds ([Elenter *et al.* 2007](#)). This approach allows using a series of layers for describing substrate gradients within the biofilm while maintaining an even distribution of particulate compounds throughout the biofilm.

External mass transfer boundary layer: Biofilms growing in virtually all full-scale biofilm reactors are subject to some degree of substrate concentration gradients external to the biofilm surface ([Lewandowski *et al.* 1994](#)). Concentration gradients external to the biofilm surface are not explicitly simulated in 1-D biofilm models. Rather, the reduction in concentration of any substrate is modelled as a mass-transfer resistance, $R_L (=L_L/D_{aq})$. The external mass-transfer resistance, R_L , is primarily dependent on biofilm reactor bulk-liquid hydrodynamics; therefore, the impact of R_L may be accounted for by using empirical correlations ([Wanner *et al.* \(2006\)](#) – see Table S4 in the supplemental material hosted at <http://www.iwaponline.com/wst/06404/0709.pdf>). A realistic description of hydrodynamic effects is ultimately dependent on an accurate estimate of the mass transfer boundary layer (MTBL) thickness, L_L . In addition, the MTBL is a mechanism that establishes a link between the

1-D biofilm model and the bulk-phase compartment, and allows the use of a 1-D biofilm model to describe a biofilm reactor. Therefore, L_L is an important facet of biofilm-reactor models that may have a substantial impact on biofilm-reactor model results and, consequently, process design. While observing a submerged fixed-bed nitrifying biofilm reactor, Zhu & Chen (2001) observed an increase in ammonium flux with a corresponding increase in Reynolds number. The researchers described changes in ammonium flux as a function of varying hydrodynamic conditions by means of a mass transfer resistance external to the biofilm – an increase in ammonium flux was associated with a decrease in the MTBL thickness. Brockmann *et al.* (2007) had to adjust the MTBL thickness to fit experimental data of a pilot-scale biofilm reactor for deammonification to model results using parameter values previously estimated in laboratory-scale batch experiments.

Diffusivity coefficients. Soluble substrates are transported into biofilms by advection and molecular diffusion. Molecular diffusion is generally considered the dominant mechanism (Zhang & Bishop 1994b). The effective diffusion coefficient value varies for different solutes (Stewart 1998). Typically, the diffusivity of a solute inside the biofilm is less than that in water because of the tortuosity of the pores and minimal biofilm permeability. Consequently, an effective diffusivity must be applied when using a mathematical biofilm model. Commonly, a value that is 80% of the solute's diffusivity in water (i.e. $D_{aq} = D_F/0.8$) is applied when modelling biofilm reactors (Wanner *et al.* 2006). Several studies have shown that diffusivity inside the biofilm decreases with biofilm depth (Zhang & Bishop 1994b; Beyenal *et al.* 1998; Beyenal & Lewandowski 2000). Decreasing diffusivity with increasing biofilm depth can be attributed to increasing density, decreasing porosity, and decreasing permeability with depth (Zhang & Bishop 1994a, b). Despite variability in the effective diffusion coefficient value, a single and constant effective diffusion coefficient value is typically used for each solute considered in biofilm models to reduce model complexity.

Parameter estimation and model calibration

Parameter estimation is a serious concern for practitioners who seek to use steady-state and/or dynamic biofilm models to describe biofilm-based processes in full-scale municipal wastewater treatment plants because most parameter values cannot be measured directly in full-scale treatment facilities (Brockmann *et al.* 2008). In addition to stoichiometric and biokinetic parameters also used in

activated sludge models, parameters exist for describing external and internal mass transfer as well as the biofilm itself. A majority of parameter values in modern process models (e.g. those described by Henze *et al.* 2000) have a substantial database that serves to define a relatively narrow range of values that are applicable to a majority of municipal wastewater treatment systems (see Hauduc *et al.* 2011). Existing biofilm models are relatively insensitive to changes in a majority of the biokinetic parameter values described by Henze *et al.* (2000) within the range of reported values. However, exceptions exist. In some cases, the mathematical description of processes consists of variable, or *lumped*, parameters. These parameter values are often system specific and subject to significant uncertainty, and account for an incomplete mechanistic description of the simulated process.

Systematic identification of parameter subsets that require definition for biofilm model calibration has been the subject of recent investigations by Smets *et al.* (1999), Van Hulle *et al.* (2004), and Brockmann *et al.* (2008). In contrast, Sin *et al.* (2008) and Bilyk *et al.* (2008) used ad hoc expert-based trial and error approaches to calibrate biofilm process models by manipulating system specific parameters related to *attachment*, *detachment*, and *biofilm thickness* (Sin *et al.* 2008) or by adjusting the 'assumed biofilm thickness' and incorporating an assimilative denitrification reaction (Bilyk *et al.* 2008). All identification and biofilm reactor model calibration efforts were based on bulk-phase measurements, but only Sin *et al.* (2008) used measured characteristics of the biofilm. Such adjustments to system specific biofilm and biokinetic parameters in order to match observed data may not produce a properly calibrated model that is capable of describing a variety of design conditions for a WWTP. Suffice it to say that a reliable and transparent description of recommended approaches for the application and calibration of biofilm models is required for the models to gain general acceptance and understanding, and be subject to consistent effective use in engineering design. Protocol defining methodology for sampling, testing, evaluating and applying data to mathematical biofilm reactor models is required. Such systematic calibration protocol exists for activated sludge models. Sin *et al.* (2005) presented a critical comparison of different calibration protocols. These protocols have many similarities that are applicable to biofilm reactor models including goal definition, data collection/verification/reconciliation, and validation. The major differences between the protocols reported by Sin *et al.* (2005) are related to the sample measurement campaign, influent wastewater characterization test methodology, and parameter subset selection and calibration. These are areas of the existing systematic calibration

protocols that will almost certainly be aggravated when creating a systematic protocol for the calibration of biofilm reactor models. When compared to a suspended growth reactor, additional tests will certainly be required to characterize the physical attributes of a system having both suspended biomass and biofilm compartments. In addition, mathematical biofilm models have more parameters than activated sludge process models. In order to have a timely and cost effective systematic approach to calibrating biofilm models, parameters related to the biofilm compartment must be estimated from bulk-phase measurements.

The goal of this paper is to present (1) a systematic evaluation of biofilm model components and critical assumptions, and (2) a local sensitivity analysis with the aim of identifying parameter subsets for biofilm reactor model calibration. The influence of factors such as biofilm thickness, organism distribution over the thickness of the biofilm, MTBL thickness, the effect of mixing conditions (completely mixed vs. plug-flow conditions), wastewater temperature, diffusion coefficients, and biokinetic parameters were evaluated using the simulation software AQUASIM.

MATERIAL AND METHODS

Biofilm and kinetic model

A 1-D biofilm model was implemented using AQUASIM (Reichert 1998). The modelling study included state variables describing soluble (S) and particulate (X) matter. The process, kinetic, and stoichiometric model was based on Activated Sludge Model No. 3 (ASM3) as described by Henze *et al.* (2000), but storage of readily biodegradable substrate was not modelled. Two types of methanol degrading heterotrophic organisms (X_{M1} and X_{M2}) were included in the model to describe tertiary denitrification using methanol as the supplemental carbon source. A complete list of state variables, stoichiometric parameters, kinetic parameters, biofilm parameters, and transformation rate expressions are listed in Tables S1–S5 in the supplemental material (<http://www.iwaponline.com/wst/06404/0709.pdf>). Biofilm detachment was modelled using two different approaches: (1) a user defined (fixed) biofilm thickness that is maintained by balancing growth and loss, and (2) using two functions describing the rate of detachment ($r_{\text{det},1} = k_{\text{det}} \cdot L_F$ and $r_{\text{det},2} = k_{\text{det}} \cdot L_F^2$). Both modelling approaches maintained a constant biofilm thickness, L_F . The rate of biofilm detachment may change depending on the assumed biofilm biomass distribution since the rate of growth and loss (in this case by endogenous

respiration) is dependent on local substrate availability and environmental conditions. Biofilm fragments were assumed to detach from the biofilm surface; therefore, preferential detachment is considered for the heterogeneous (layered) biofilm biomass distribution (i.e. bacteria growing at the biofilm–liquid interface detach from the biofilm surface and enter the bulk of the liquid). Substrate concentration gradients external to the biofilm were modelled as a mass transfer resistance using the concept of a MTBL with thickness L_L . Results reported for all but one of the models describe partially penetrated biofilms (i.e. the rate-limiting substrate is exhausted before reaching the growth medium; therefore, the biofilm is not biomass limited). The tertiary nitrification MBBR (with a biofilm thickness of 67 μm) was biomass limited, or completely penetrated.

Simulations

Municipal wastewater treatment scenarios that are commonly the subject of full-scale process design and evaluation were modelled including combined carbon oxidation and nitrification, tertiary nitrification, and tertiary denitrification. The submerged, completely mixed biofilm reactors are described as continuous flow stirred tank reactors (CFSTRs) analogous to moving bed biofilm reactors (MBBRs). In addition, an integrated fixed film activated sludge (IFAS) process for combined carbon oxidation and nitrification was modelled. Influent wastewater characteristics and reactor configurations are defined in Table 1. The influent wastewater characteristics were developed based on selected references and authors' experience with the simulation and design of these processes. The influent wastewater flow rate for each case modelled was 35,000 m^3/d . Reactor configurations were defined based on (1) design criteria presented by Boltz *et al.* (2010a) and McQuarrie & Boltz (2011), describing combined carbon oxidation and nitrification MBBR, tertiary nitrification MBBR, and tertiary denitrification MBBR, and (2) a requirement that less than 1 mg methanol/L remained in the tertiary denitrification MBBR effluent stream. IFAS process design was created based on author experience, which has been presented to a certain extent by Kim *et al.* (2010). Steady-state simulations were run for 20 °C unless otherwise stated, a representative annual average day temperature.

Table 2 provides a summary of the different modelling scenarios used to quantify the impact of changes in biofilm thickness, biofilm structure, MTBL thickness, mixing conditions, temperature, and model parameter values in general. A homogeneous biofilm structure was modelled by introducing an artificial diffusion coefficient of all particulate compounds (Elenter *et al.* 2007). The value of the diffusion

Table 1 | Reactor configurations and wastewater characteristics for the simulated municipal wastewater treatment scenarios

	Configurations			
	(A) MBBR Combined carbon oxidation and nitrification	(B) MBBR Tertiary nitrification	(C) MBBR Tertiary denitrification	(D) IFAS Combined carbon oxidation and nitrification
<i>Reactor configuration</i>				
Reactor volume (m ³)	5,000	2,200	1,400	2,200
Biofilm surface area (m ²)	1,250,000	550,000	350,000	550,000
Bulk phase DO (mg O ₂ /L)	4.0	5.0	0.0	4.0
Influent flow rate (m ³ /d)	35,000	35,000	35,000	35,000
<i>Wastewater characteristics</i>				
S _S (g COD/m ³)	89.0	5.7	1.1	40.0
S _M (g COD/m ³)	–	–	15.0	–
S _I (g COD/m ³)	13.3	18.7	18.7	13.3
S _{NH4} (g N/m ³)	26.0	22.5	2.0	26.0
S _{NO3} (g N/m ³)	0.7	1.4	5.1	0.7
S _{ALK} (mol HCO ₃ ⁻ /m ³)	4.8	5.0	4.1	4.8
X _S (g COD/m ³)	250.0	0.2	8.3	250.0
X _I (g COD/m ³)	69.3	2.1	2.1	69.3

Table 2 | Modelling scenarios (base scenario settings are underlined)

Scenarios	Parameter	Values evaluated		
I	Biofilm thickness, L_F	<u>Fixed thickness (200 μm)</u>	Deep biofilm (2,000 μm)	L_F resulting from different detachment rate functions
II	Biofilm structure	<u>Heterogeneous (layered)</u>	Homogeneous	
III	MTBL thickness, L_L	<u>$L_L = 100 \mu\text{m}$</u>	$L_L = 0 \mu\text{m}$	$L_L = L_c/\text{Sh}^a$
IV	Reactors-in-series	<u>$N = 1$</u>	$N = 3$	$N = 6$
V	Temperature	<u>20 °C</u>	12 °C	
VI	Parameter values	From Table S9 in the Appendix (Sensitivity analysis)		

^aMass transfer boundary layer (MTBL) thickness L_L calculated for each soluble substance individually with L_c being the characteristic length and Sh the Sherwood number (for details see Appendix S4 in the Supplemental Material <http://www.iwaponline.com/wst/06404/0709.pdf>).

coefficient for particulate compounds was assigned a great enough value to guarantee that no significant gradient for these particulate compounds could develop over the biofilm thickness. The influence of parameter values (scenario VI) was analysed based on local sensitivity analyses at 20 and 12 °C. The local sensitivity analysis approach used is described in more detail below.

Local sensitivity analysis

Model sensitivity to changes in biokinetic and biofilm parameter values was evaluated for steady state and discussed

with emphasis given to identifying the parameters that may have a negligible impact on model results when adjusting the values within a range reported in the literature. Parameter values that may vary from system to system treating municipal wastewater (e.g. $K_{O_2,A}$, L_F) are identified and the impact of changes in their values (again within a range of values reported in the literature) is evaluated. Although parameter values may vary considerably, model sensitivity was not evaluated based on a global sensitivity analysis as described in Brockmann *et al.* (2008), but on a simpler local sensitivity analysis. While the global sensitivity analysis accounts for non-linear model outcomes within the

defined uncertainty ranges of the parameters, the local sensitivity analysis linearly extrapolates the impact of a small change in the parameter value to the uncertainty range of the parameter. Local sensitivity analyses were carried out for the base scenario altering the parameters in incremental steps defined by 1% of their default value. A sensitivity measure δ was calculated from scaled sensitivity values that include information on a reasonable range (i.e. the uncertainty range) of the parameters (Brun *et al.* 2001):

$$\delta = \sqrt{\frac{1}{n} \sum_{i=1}^n s_{i,j}^2} \quad \text{with} \quad s_{i,j} = \frac{\Delta p_j}{sc_i} \cdot \frac{\partial y_i}{\partial p_j}$$

where Δp_j represents the uncertainty range of the parameter p_j , sc_i is a scale factor, and n is the number of model outputs considered. A large δ means that a change of Δp_j in parameter p_j has a substantial impact on the considered model output(s). Model parameters were assigned to three uncertainty classes according to Brun *et al.* (2002). In this study, sensitivity analyses were only carried out for parameters from uncertainty classes 2 and 3. Parameters from uncertainty class 1 were not considered for sensitivity analysis due to their low uncertainty (or 5% of the default parameter value) when compared to uncertainty classes 2 and 3. The uncertainty range of parameters from uncertainty class 2 is 20% of the default parameter value, and 50% for parameters from uncertainty class 3. Studied parameters and their uncertainty ranges are given as supplemental material <http://www.iwaponline.com/wst/06404/0709.pdf>.

RESULTS AND DISCUSSION

Benchmark simulations

The influence of biofilm thickness (scenario I), biofilm structure (scenario II), MTBL thickness (scenario III), mixing conditions (scenario IV), temperature (scenario V), and specific parameter values (scenario VI) were evaluated, as summarized in Table 2, for the different reactor configurations described in Table 1. Table 3 lists results for the combined carbon oxidation and nitrification MBBR simulations (i.e., configuration A), Table 4 lists results from tertiary nitrification MBBR simulations (i.e. configuration B), Table 5 lists results from tertiary denitrification MBBR simulations (i.e. configuration C), and Table 6 lists results from IFAS process simulations (i.e. configuration D).

Biofilm thickness (scenario I): Model results obtained from simulating a submerged and completely mixed combined carbon oxidation and nitrification biofilm reactor (e.g. the MBBR described as configuration A in Table 3) indicated that the nitrate (S_{NO_3}) and slowly biodegradable organic matter (X_S) concentrations remaining in the effluent stream were less when the biofilm was thicker (e.g. $L_F = 2,000 \mu\text{m}$). In contrast, the readily biodegradable organic matter (S_S), ammonium (S_{NH_4}), and di-nitrogen (S_{N_2}) concentrations remaining in the effluent stream were less when the biofilm was thinner (e.g. $L_F = 200 \mu\text{m}$). As the bulk-liquid S_{NO_3} and S_{N_2} concentrations are a measure of denitrification, it follows that denitrification rates were greater when the biofilm was thicker. In systems with thinner biofilms (e.g. $L_F = 200 \mu\text{m}$), denitrification was inhibited by the presence of oxygen, or limited by the availability of substrate or biomass. In addition, the hydrolysis of X_S to S_S was limited by the available mass of non-methanol degrading heterotrophic bacteria (X_H) in thinner biofilms (e.g. $L_F = 200 \mu\text{m}$). Thus, the biofilm thickness had an impact on denitrification in the biofilm and the extent of hydrolysis. Greater S_S and S_{NH_4} concentrations remaining in the effluent stream of the simulated MBBR with thicker biofilms (e.g. $L_F = 2,000 \mu\text{m}$) resulted from increased hydrolysis of X_S to S_S and dissolved oxygen limited aerobic conversion processes. Bulk-liquid substrate concentrations and substrate fluxes did not vary with biofilm thickness according to the tertiary nitrification and tertiary denitrification MBBR model results (as described by configurations B and C) (see Tables 4 and 5). The model results are in agreement with experimental observations reported by others. Okabe *et al.* (2002) observed for an autotrophic nitrifying biofilm that dissolved oxygen diffusing into the biofilm was depleted approximately $150 \mu\text{m}$ from the biofilm surface, ammonium and nitrite were both converted to nitrate within $100 \mu\text{m}$ of the biofilm surface, and ammonia oxidizing bacteria (AOB) and nitrite oxidizing bacteria (NOB) were densely present inside $100 \mu\text{m}$ (from the liquid-biofilm interface). Similarly, Schramm *et al.* (1996) observed dense populations of AOB and NOB in the upper and aerobic $100 \mu\text{m}$ (from the liquid-biofilm interface) of a nitrifying biofilm. Horn & Hempel (1995) observed for both autotrophic and heterotrophic biofilms that oxygen was depleted within $100\text{--}200 \mu\text{m}$ of the liquid-biofilm interface. Therefore, it may be deduced that for aerobic conversion processes, such as nitrification, biofilm thicknesses greater than approximately $200 \mu\text{m}$ do not influence substrate concentrations (remaining in the effluent stream) and substrate fluxes as only the upper aerobic part of the biofilm

Table 3 | Steady state simulation results for combined carbon oxidation and nitrification in an MBBR (configuration A)

Scenario	S_{NH_4} (g N/m ³ , g COD/m ³)	S_{O_2}	S_{NO_3}	S_s	X_s	S_{N_2}	J_{NH_4} (g N/(m ² · d), g COD/(m ² · d))	J_{NO_3}	J_s	J_{O_2}	J_{X_s}	J_{N_2}
<i>Scenario I: Impact of altering biofilm thickness and detachment model</i>												
$L_F = 200 \mu\text{m}$, 10 layers ^a	1.4	4.0	20.3	3.2	223.2	1.5	0.63	-0.53	1.88	3.51	0.13	-0.04
$L_F = 2,000 \mu\text{m}$, 10 layers	8.6	4.0	4.3	5.4	203.7	11.5	0.46	-0.09	2.03	2.99	1.06	-0.33
$L_F = 2,000 \mu\text{m}$, 60 layers ^c	2.7	4.0	12.8	3.6	202.8	8.2	0.62	-0.32	2.08	3.62	1.02	-0.23
$L_F = 197 \mu\text{m}$, 10 layers ^b	1.4	4.0	20.3	3.2	223.3	1.5	0.63	-0.53	1.87	3.50	0.13	-0.04
$L_F = 1,241 \mu\text{m}$, 60 layers ^c	2.4	4.0	16.6	3.4	210.0	4.4	0.61	-0.42	1.98	3.59	0.69	-0.12
<i>Scenario II: Impact of assumed biofilm biomass distribution</i>												
Heterogeneous ^a	1.4	4.0	20.3	3.2	223.2	1.5	0.63	-0.53	1.88	3.51	0.13	-0.04
Homogeneous	2.3	4.0	19.7	3.3	225.6	1.7	0.60	-0.51	1.94	3.61	0.13	-0.04
<i>Scenario III: Impact of altering mass transfer boundary layer thickness</i>												
$L_L = 100 \mu\text{m}$ ^a	1.4	4.0	20.3	3.2	223.2	1.5	0.63	-0.53	1.88	3.51	0.13	-0.04
$L_L = 0 \mu\text{m}$	0.8	4.0	21.6	1.6	223.3	0.7	0.67	-0.58	2.32	3.86	0.13	-0.02
$L_L = L_c/Sh^d$	1.1	4.0	21.1	2.3	223.3	1.0	0.65	-0.56	2.09	3.70	0.13	-0.03
<i>Scenario IV: Impact of mixing regime on model results for N continuous flow stirred tank reactors-in-series (CFSTR vs. plug-flow)</i>												
$N = 1$ ^a	1.4	4.0	20.3	3.2	223.2	1.5	0.63	-0.53	1.88	3.51	0.13	-0.04
$N = 3$	0.5	4.0	20.3	0.6	224.2	2.3	0.67	-0.53	2.20	3.61	0.11	-0.06
$N = 6$	0.2	4.0	20.7	0.6	224.9	2.0	0.69	-0.54	2.33	3.67	0.11	-0.05
<i>Scenario V: Impact of altering temperature</i>												
$T = 20 \text{ }^\circ\text{C}$ ^a	1.4	4.0	20.3	3.2	223.2	1.5	0.63	-0.53	1.88	3.51	0.13	-0.04
$T = 12 \text{ }^\circ\text{C}$	6.6	4.0	14.9	4.6	230.6	1.6	0.50	-0.39	2.01	2.81	0.10	-0.04

^aBase scenarios are underlined.

^b $k_{\text{detach}} \cdot L_F$ with $k_{\text{detach}} = 0.2 \text{ (1 d}^{-1}\text{)}$.

^c $k_{\text{detach}} \cdot L_F^2$ with $k_{\text{detach}} = 30 \text{ (1 d}^{-1} \text{ m}^{-1}\text{)}$.

^dSupplemental material S4, <http://www.iwaponline.com/wst/06404/0709.pdf>. Calculated values: L_{L,NH_4} : 51 μm , L_{L,NO_3} : 50 μm , $L_{L,SS}$: 43 μm , $L_{L,XS}$: 36 μm , L_{L,O_2} : 55 μm , $L_{L,ALK}$: 43 μm .

^eSimulations with 100 layers resulted in numerical instability.

will substantially contribute to the conversion processes. However, when aerobic and anoxic conversion processes are desirable in the same biofilm, biofilm thickness has a distinct impact on substrate concentrations (remaining in the effluent stream) and substrate fluxes. In thin, yet partially penetrated, biofilms (e.g. $L_F < 100\text{--}200 \mu\text{m}$), primarily aerobic conditions will prevail where thicker biofilms (e.g. $L_F > 200 \mu\text{m}$) are able to sustain the development of both aerobic and anoxic zones. Therefore, if simultaneous nitrification and denitrification are desired in a single-stage biofilm reactor then the reactor should be operated in a manner that promotes the development of thicker biofilms (e.g. $L_F > 200 \mu\text{m}$). In contrast, if a low ammonium concentration (remaining in the effluent stream) is desired, then operating conditions that promote the development of thin biofilms (e.g. $L_F < 100\text{--}200 \mu\text{m}$) are desirable to ensure that biofilm surface area and dissolved oxygen penetration inside the biofilm are simultaneously maximized.

Simulations were carried out describing a 2,000- μm thick biofilm to evaluate the influence of biofilm discretization on model results when assuming that a heterogeneous 1-D biofilm structure is described as a series of parallel layers. Specifically, the models were used to quantify the impact that a different number of layers would have on simulation results. Modelling combined carbon oxidation and nitrification in a MBBR and discretizing the 1-D biofilm with relatively few layers (i.e. 10 layers) resulted in lower carbon and ammonium fluxes and a higher denitrification rate when compared to results from a model in which the 1-D biofilm was discretized with a greater number of layers (i.e. 60 layers) (Table 3). The difference in model results can be explained by the poorly approximated substrate and biomass gradients over the biofilm depth when dividing the biofilm into relatively few layers. The numerical methodology typically used to calculate a concentration gradient, or gradients, in 1-D biofilm models that discretize the biofilm

Table 4 | Steady state simulation results for tertiary nitrification in an MBBR (configuration B)

Scenario	S_{NH4} (g N/m ³)	S_{O2} (g COD/m ³)	S_{NO3}	S_S	X_S	S_{N2}	J_{NH4} (g N/(m ² · d))	J_{NO3} (g COD/(m ² · d))	J_S	J_{O2}	J_{XS}	J_{N2}
<i>Scenario I: Impact of altering biofilm thickness and detachment model</i>												
<u>$L_F = 200 \mu\text{m}$, 10 layers^a</u>	1.9	5.0	21.4	0.7	7.8	0.3	1.29	-1.25	0.32	5.79	0.00	-0.02
$L_F = 2,000 \mu\text{m}$, 10 layers, actual L_F 864 μm	2.6	5.0	20.5	0.8	7.6	0.5	1.26	-1.21	0.32	5.65	0.02	-0.03
$L_F = 2,000 \mu\text{m}$, 100 layers, actual L_F 877 μm	1.9	5.0	21.4	0.7	7.6	0.3	1.29	-1.25	0.32	5.80	0.02	-0.02
$L_F = 67 \mu\text{m}$, 10 layers ^b	2.1	5.0	21.3	0.7	7.8	0.1	1.27	-1.24	0.32	5.67	0.00	-0.01
$L_F = 622 \mu\text{m}$, 30 layers ^c	1.9	5.0	21.4	0.7	7.7	0.3	1.29	-1.25	0.32	5.80	0.01	-0.02
<i>Scenario II: Impact of assumed biofilm biomass distribution</i>												
<u>Heterogeneous^a</u>	1.9	5.0	21.4	0.7	7.8	0.3	1.29	-1.25	0.32	5.79	0.00	-0.02
Homogeneous	1.9	5.0	21.0	0.7	7.8	0.7	1.29	-1.23	0.32	5.80	0.00	-0.05
<i>Scenario III: Impact of altering mass transfer boundary layer thickness</i>												
<u>$L_L = 100 \mu\text{m}$^a</u>	1.9	5.0	21.4	0.7	7.8	0.3	1.29	-1.25	0.32	5.79	0.00	-0.02
$L_L = 0 \mu\text{m}$	0.8	5.0	22.7	0.4	7.8	0.1	1.36	-1.34	0.35	6.19	0.00	-0.01
$L_L = L_c/Sh^d$	1.3	5.0	22.2	0.6	7.8	0.2	1.33	-1.30	0.34	6.03	0.00	-0.01
<i>Scenario IV: Impact of mixing regime on model results for N continuous flow stirred tank reactors-in-series (CFSTR vs. plug-flow)</i>												
<u>$N = 1$^a</u>	1.9	5.0	21.4	0.7	7.8	0.3	1.29	-1.25	0.32	5.79	0.00	-0.02
$N = 3$	1.0	5.0	22.2	0.3	7.7	0.5	1.35	-1.30	0.35	6.01	0.00	-0.03
$N = 6$	0.5	5.0	22.5	0.2	7.7	0.5	1.38	-1.33	0.36	6.12	0.00	-0.03
<i>Scenario V: Impact of altering temperature</i>												
<u>$T = 20 \text{ }^\circ\text{C}$^a</u>	1.9	5.0	21.4	0.7	7.8	0.3	1.29	-1.25	0.32	5.79	0.00	-0.02
$T = 12 \text{ }^\circ\text{C}$	6.1	5.0	17.2	0.9	7.9	0.3	1.03	-0.99	0.31	4.59	0.00	-0.02

^aBase scenarios are underlined.^b $K_{detach} \cdot L_F$.^c $K_{detach} \cdot L_F^2$.^dSupplemental material S4, <http://www.iwaponline.com/wst/06404/0709.pdf>. Calculated values: $L_{L,NH4}$: 51 μm , $L_{L,NO3}$: 50 μm , $L_{L,SS}$: 43 μm , $L_{L,XS}$: 36 μm , $L_{L,O2}$: 55 μm , $L_{L,ALK}$: 43 μm .

into a series of layers (having an equal thickness) results in a straight line between the midpoints of each layer. As such, consider an extreme in which a 1-D biofilm model consists of only one layer. The concentration profile would be a straight line, which differs substantially from the curved reduction typical of biofilms. Therefore, when simulating thick mixed-culture biofilms with a low discretization (e.g. 1,000- μm thick biofilm with 10 layers resulting in 100- μm thick layers), the user must be aware that the biofilm model will likely not properly reflect substrate and, consequently, biomass gradients in the biofilm, and accurate system simulations will not result. Discussions held during the *WWTmod 2010* (Monte Sainte Anne, Canada) biofilm modelling workshop suggested that it was a typical practice of 'industry' professionals to decrease the number of layers (e.g. to three to five) when modelling a heterogeneous 1-D biofilm. Generally, this measure was taken to reduce simulation time. As demonstrated with the series of layers (in

this study having equal thickness) approach and supporting model results presented in this paper, the use of too few layers may impair such a model's ability to generate accurate results. The following section on biofilm structure describes conditions in which the loss of spatial resolution will in fact impair model ability to generate accurate results.

After comparing model results no significant variation in bulk-liquid substrate concentrations or material fluxes were observed from the two different biofilm detachment modelling approaches that were applied in this study. Both modelling approaches maintained a constant biofilm thickness, L_F . The rate of detachment changed depending on the assumed biofilm biomass distribution since the rate of growth and loss (in this case by endogenous respiration) is dependent on local substrate availability and environmental conditions. Model results can be reviewed for the combined carbon oxidation and nitrification MBBR, tertiary nitrification MBBR, and tertiary denitrification MBBR in [Tables 3–5](#), respectively.

Table 5 | Steady state simulation results for tertiary denitrification with methanol in an MBBR (configuration C)

Scenario	S_{NH_4} (g N/m ³ , g COD/m ³)	S_{NO_3}	S_s	S_m	X_s	S_{N_2} (g N/(m ² · d), g COD/(m ² · d))	J_{NH_4}	J_{NO_3}	J_s	J_m	J_{X_s}	J_{N_2}
<i>Scenario I: Impact of altering biofilm thickness and detachment model</i>												
<u>$L_F = 200 \mu\text{m}$, 10 layers^a</u>	1.6	2.0	0.3	1.4	0.2	3.1	0.04	0.30	0.08	1.33	0.00	-0.30
$L_F = 2,000 \mu\text{m}$, 10 layers	1.7	1.9	0.3	1.6	0.2	3.2	0.04	0.35	0.08	1.45	0.00	-0.35
$L_F = 2,000 \mu\text{m}$, 100 layers	1.6	1.8	0.2	0.6	0.2	3.3	0.04	0.33	0.09	1.43	0.00	-0.33
$L_F = 110 \mu\text{m}$, 10 layers ^b	1.6	2.0	0.3	1.4	0.2	3.1	0.04	0.30	0.08	1.32	0.00	-0.30
$L_F = 848 \mu\text{m}$, 40 layers ^c	1.6	2.0	0.3	1.4	0.2	3.1	0.04	0.30	0.08	1.33	0.00	-0.30
<i>Scenario II: Impact of assumed biofilm biomass distribution</i>												
<u>Heterogeneous^a</u>	1.6	2.0	0.3	1.4	0.2	3.1	0.04	0.30	0.08	1.33	0.00	-0.30
Homogeneous	1.6	1.9	0.3	1.4	0.2	3.2	0.03	0.31	0.07	1.33	0.00	-0.31
<i>Scenario III: Impact of altering mass transfer boundary layer thickness</i>												
<u>$L_L = 100 \mu\text{m}$^a</u>	1.6	2.0	0.3	1.4	0.2	3.1	0.04	0.30	0.08	1.33	0.00	-0.30
$L_L = 0 \mu\text{m}$	1.6	1.8	0.2	0.5	0.2	3.3	0.04	0.32	0.08	1.42	0.00	-0.32
$L_L = L_c/Sh^d$	1.6	1.9	0.3	1.0	0.2	3.2	0.04	0.31	0.08	1.37	0.00	-0.31
<i>Scenario IV: Impact of mixing regime on model results for N continuous flow stirred tank reactors-in-series (CFSTR vs. plug-flow)</i>												
<u>$N = 1$^a</u>	1.6	2.0	0.3	1.4	0.2	3.1	0.04	0.30	0.08	1.33	0.00	-0.30
$N = 3$	1.6	1.8	0.2	0.2	0.2	3.3	0.04	0.33	0.09	1.45	0.00	-0.33
$N = 6$	1.6	1.8	0.1	0.0	0.2	3.4	0.04	0.33	0.09	1.47	0.00	-0.33
<i>Scenario V: Impact of altering temperature</i>												
<u>$T = 20 \text{ }^\circ\text{C}$^a</u>	1.6	2.0	0.3	1.4	0.2	3.1	0.04	0.30	0.08	1.33	0.00	-0.30
$T = 12 \text{ }^\circ\text{C}$	1.7	2.1	0.4	2.1	0.2	3.0	0.03	0.29	0.07	1.27	0.00	-0.29

^aBase scenarios are underlined.^b $k_{\text{detach}} \cdot L_F$.^c $k_{\text{detach}} \cdot L_F^2$.^dSupplemental material S4, <http://www.iwaponline.com/wst/06404/0709.pdf>. Calculated values: L_{L,NH_4} : 51 μm , L_{L,NO_3} : 50 μm , $L_{L,SS}$: 43 μm , L_{L,X_s} : 36 μm , L_{L,O_2} : 55 μm , $L_{L,ALK}$: 43 μm .**Table 6** | Steady state simulation results for carbon oxidation and nitrification in the IFAS (configuration D)

Scenario	S_{NH_4} (g N/m ³ , g COD/m ³)	S_{O_2}	S_{NO_3}	S_s	X_s	S_{N_2}	J_{NH_4} (g N/(m ² · d), g COD/(m ² · d))	J_{NO_3}	J_s	J_{O_2}	J_{X_s}	J_{N_2}
<i>Scenario III: Impact of altering mass transfer boundary layer thickness</i>												
<u>$L_L = 100 \mu\text{m}$^a</u>	2.4	4.0	22.7	0.4	220.2	0.4	1.02	-1.00	0.06	4.44	0.02	0.00
$L_L = 0 \mu\text{m}$	1.5	4.0	23.6	0.4	220.3	0.4	1.21	-1.18	0.42	5.44	0.04	0.00
$L_L = L_c/Sh^b$	1.8	4.0	23.2	0.4	220.2	0.4	1.14	-1.12	0.13	5.00	0.03	0.00
<i>Scenario V: Impact of altering temperature</i>												
<u>$T = 20 \text{ }^\circ\text{C}$^a</u>	2.4	4.0	22.7	0.4	220.2	0.4	1.02	-1.00	0.06	4.44	0.02	0.00
$T = 12 \text{ }^\circ\text{C}$	19.1	4.0	6.1	0.7	229.3	0.3	0.21	-0.20	0.12	0.95	0.01	0.00

^aBase scenarios are underlined.^bSupplemental material S4, <http://www.iwaponline.com/wst/06404/0709.pdf>. Values: L_{L,NH_4} : 51 μm , L_{L,NO_3} : 50 μm , $L_{L,SS}$: 43 μm , L_{L,X_s} : 36 μm , L_{L,O_2} : 55 μm , $L_{L,ALK}$: 43 μm .

Biofilm structure (scenario II): Simulation of combined carbon oxidation and nitrification in mixed-culture biofilms (configuration A) assuming a homogeneous biofilm biomass

distribution resulted in significantly different simulation results for effluent S_{NH_4} , while all other concentrations predicted by the model, including ammonium flux, were not

significantly affected when compared to simulation results from a model that assumed a heterogeneous biofilm biomass distribution (Table 3). In contrast, the biofilm biomass distribution did not affect simulation results in a submerged and completely mixed biofilm reactor such as a tertiary nitrification MBBR (Table 4) and tertiary denitrification MBBR (Table 5) (configurations B and C).

Elenter *et al.* (2007) stated that a heterogeneous (layered) 1-D biofilm model overpredicted the negative impact of heterotrophic bacteria overgrowing autotrophic nitrifying bacteria. However, it has been observed experimentally that mixed-culture biofilms in combined carbon oxidation and nitrification bioreactors primarily consist of heterotrophic bacteria near the bulk liquid and biofilm interface while autotrophic nitrifiers tend to exist closer to the growth medium (Okabe *et al.* 1995). This observation has led to the biofilm being discretized as a series of layers in each of the heterogeneous 1-D biofilm models in this study. The same approach was applied to the referenced work by Wanner *et al.* (2006) and Elenter *et al.* (2007). However, systematic deviations between observed and simulated ammonium flux values prompted Elenter *et al.* (2007) to question model results when using a layering approach to describe heterogeneous biofilms. Autotrophic nitrifiers growing in mixed-culture biofilms have a propensity to develop in dense clusters that form microcolonies (Okabe *et al.* 1999; Kindaichi *et al.* 2004). These clusters of autotrophic nitrifiers may develop close to the biofilm surface and result in an ammonium flux that is greater than values obtained from the aforementioned heterogeneous (layered) 1-D biofilm model. Elenter *et al.* (2007) used this experimental observation to explain why the heterogeneous (layered) 1-D biofilm model was underpredicting ammonium flux while the homogeneous 1-D biofilm model had the ability to describe observed ammonium flux well in an experimental submerged biofilm reactor operating with conditions similar to the hypothetical tertiary nitrifying MBBR described in Table 1.

The assumption of a homogeneous biofilm biomass distribution does not explicitly account for the impact that spatial variability has on modelled flux value(s). However, the autotrophic nitrifiers are exposed to a greater dissolved oxygen concentration as they are allowed to develop closer to the bulk-liquid and biofilm interface. On the other hand, the nitrifier concentration is 'diluted' as a result of being distributed throughout the entire biofilm thickness. In effect, the relative abundance of biofilm entrained organism(s) is the same throughout the biofilm depth. For this reason, one can mathematically model the influence that (primarily soluble) organic matter will have on the modelled ammonium flux

by assuming either a heterogeneous (layered) or homogeneous biofilm biomass distribution. A 1-D biofilm model, independent of the assumed biofilm structure applied to the simulations (i.e. heterogeneous or homogeneous biofilm biomass distribution), that properly accounts for competition inside the biofilm will negate the impact that biofilm thickness has on modelled substrate flux values when simulating a partially penetrated, or thick, biofilm. Essentially, the 'active' aerobic portion of the biofilm (which extends into the biofilm from the liquid-biofilm interface) will be defined by rate-limiting substrate availability (e.g. dissolved oxygen or ammonium). The depth of its penetration into the biofilm will have the most significant impact on the extent of activity. Increasing biofilm thickness beyond the rate-limiting substrate penetration depth will not increase flux. Rather, inert material will accumulate near the biofilm-growth medium interface, or anoxic/anaerobic processes will occur.

MTBL thickness (scenario III), mixing conditions (scenario IV), and temperature (scenario V): Concentration gradients external to the biofilm surface, which has been modelled as an external mass transfer resistance (scenario III), have a substantial effect on modelled substrate flux values. The general trend is an increasing substrate flux with decreasing MTBL thickness due to the increased substrate concentration at the liquid-biofilm interface and resulting increased driving force. Increasing the MTBL thickness from 0 to 100 μm resulted in an ammonium flux (J_{NH_4}) decreasing 6, 5, 7, and 16% for configurations A, B, C, and D, respectively. Alternatively, increasing the MTBL thickness from 0 to 100 μm resulted in the flux of readily biodegradable organic matter (J_{S}) changing 19, 9, 11, and 85% for configurations A, B, C, and D, respectively. To place the changes in perspective, varying MTBL thickness from 0 to 100 μm resulted in S_{NH_4} decreasing 175, 238, 8, and 160% for configurations A, B, C, and D, respectively, while the same change in MTBL thickness resulted in S_{S} varying 200, 175, 280, and 0% also for configurations A, B, C, and D, respectively. Uncertainty imposed (when using biofilm models to describe biofilm reactor performance) by variability in MTBL thickness has been well documented by Boltz & Daigger (2010). These results agree with those presented by Zhu & Chen (2001), who observed that the ammonium flux in a nitrifying biofilm reactor significantly increased with decreasing MTBL thickness.

Increasing the number of completely mixed, submerged biofilm reactors-in-series (scenario IV) improved the simulated system removal efficiency, and resulted in lower effluent substrate concentrations for S_{S} , S_{NH_4} , S_{NO_3} , and S_{M} . The observed behaviour is in accordance with reaction

kinetics through equally sized reactors-in-series (e.g. Rittmann & McCarty 2001). Temperature (scenario V) not only affects biochemical transformation (including growth and endogenous respiration) rates but also the diffusivity of any soluble substance. Carbon oxidation, nitrification, and denitrification efficiencies decreased with decreasing temperature. The increase in soluble substance diffusivity was accounted for by applying a temperature dependence relationship to the diffusion coefficients (Table S4 in the supplemental material, <http://www.iwaponline.com/wst/06404/0709.pdf>). Low temperatures (e.g. 12 °C) influenced nitrification to a greater extent than carbon oxidation and denitrification in the modelled biofilm reactors.

In addition to submerged, completely mixed biofilm reactors for different wastewater treatment scenarios, a combined carbon oxidation and nitrification IFAS system was also modelled (configuration D). The simulation results are summarized in Table 6. The mixed liquor suspended solids (MLSS) concentration was approximately 2,800 g m⁻³. In the IFAS process, organic carbon was primarily oxidized by non-methanol degrading heterotrophic bacteria in the suspended growth compartment. Only 2% of carbon oxidation took place in the biofilm, resulting in a higher ammonium flux (when compared with the combined carbon oxidation and nitrification MBBR). The rate of nitrification in the combined carbon oxidation and nitrification MBBR (configuration A) is less than that observed in the IFAS process, as autotrophic nitrifiers must compete with non-methanol degrading heterotrophic bacteria for space in the biofilm and for the electron acceptor, namely dissolved oxygen.

Sensitivity analysis – specific parameter values (scenario VI)

Sensitivity measures δ for biokinetic and biofilm parameter values are presented in Figures 1 and 2 for IFAS and three municipal wastewater treatment scenarios based on MBBR technology. Results presented in Figure 1 are for 20 °C and in Figure 2 for 12 °C. The sensitivity measure δ was calculated for each parameter based on sensitivity values for S_{NH_4} , S_{NO_3} and S_{S} concentrations, and sensitivity values for fluxes of ammonium, nitrate, soluble organic substrate in combined carbon oxidation and nitrification MBBR (configuration A), tertiary nitrification MBBR (configuration B), and combined carbon oxidation and nitrification IFAS (configuration D) processes. For tertiary denitrification (configuration C), δ was calculated based on sensitivity values for bulk-liquid nitrate, soluble organic substrate, and methanol concentrations, and sensitivity values for fluxes of nitrate,

organic substrate, methanol and di-nitrogen. The parameters having the most substantial impact on model results depend on the treatment system under study and the selected model outputs. For combined carbon oxidation and nitrification, μ_{H} and $K_{\text{S,H}}$ had a large influence on bulk-liquid concentrations and fluxes through the biofilm surface pointing to a large influence of carbon oxidation on nitrification due to competition between heterotrophic and autotrophic organisms inside the biofilm (Figure 1). This is in agreement with the findings of Wanner & Gujer (1984), who demonstrated that autotrophic nitrifier activity in a combined carbon oxidation and nitrification biofilm is highly influenced by the activity of heterotrophic organisms. The MTBL thickness and dissolved oxygen diffusion coefficient affected model results and show that dissolved oxygen supply is critical. The dissolved oxygen rate limitation in aerobic biofilms has been illustrated with a variety of dissolved oxygen profile measurements which demonstrate that dissolved oxygen is commonly depleted within the upper 100–200 μm of the biofilm (Horn & Hempel 1995; Okabe *et al.* 2002). For tertiary nitrification, the MTBL thickness had the greatest impact on bulk-liquid concentrations followed by the diffusion coefficient for dissolved oxygen (which is typically the rate-limiting substrate for nitrification). Similar results were obtained in a global sensitivity analysis that evaluated two-step nitrification in a biofilm (Brockmann & Morgenroth 2007). Denitrification in a tertiary biofilm reactor model is primarily driven by the MTBL thickness and the methanol diffusion coefficient (an external carbon source which is typically the rate-limiting substrate for denitrification). Biofilm models describing a combined carbon oxidation and nitrification IFAS process were primarily impacted by the biokinetic parameters μ_{A} , μ_{H} , k_{H} , and $K_{\text{S,H}}$ and the MTBL thickness. Diffusion coefficients had a minor impact on model results. At 12 °C model results for the combined carbon oxidation and nitrification IFAS process simulation were extremely sensitive to changes in the parameters μ_{A} and $K_{\text{O}_2,\text{A}}$ (Figure 2).

Independent of the biofilm system under investigation, the MTBL thickness markedly influenced model results for each of the three biofilm systems evaluated in this study (configurations A, B, and C). The dissolved oxygen diffusion coefficient significantly impacted model results when describing aerobic biofilm systems. Similarly, the methanol diffusion coefficient impacted model outputs when describing a denitrification biofilm system. Dissolved oxygen and methanol (or another external carbon source) are typically the rate-limiting substrate in tertiary nitrification and tertiary denitrification biofilm reactors,

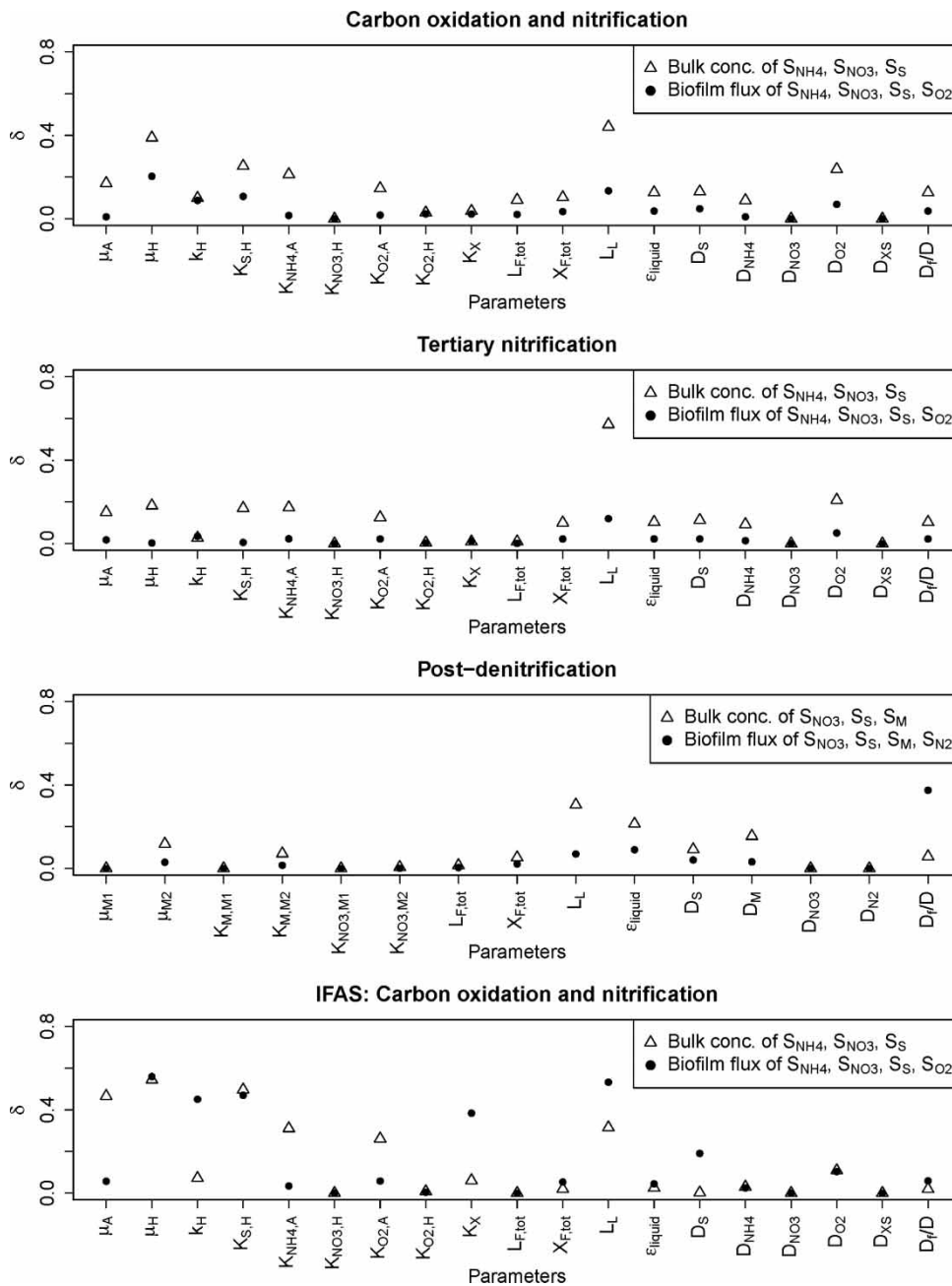


Figure 1 | Sensitivity measures δ for biokinetic and biofilm parameters for simulations at 20 °C (Scenario VI). For combined carbon oxidation and nitrification, tertiary nitrifications, and IFAS, δ is given for bulk concentrations of ammonium, nitrate and organic carbon (together), and fluxes of ammonium, nitrate, organic carbon, and oxygen (together). For tertiary denitrification, δ is given for bulk concentrations of nitrate, organic carbon, and methanol (together), and fluxes of nitrate, organic carbon, methanol, and di-nitrogen.

respectively. The MTBL thickness and aforementioned diffusion coefficients are important biofilm model parameters. Generally, these parameter values are succeeded by biokinetic parameters pertaining to the dominating organism species inside the biofilm, which is typically the slowest growing organism species when modelling IFAS processes.

CONCLUSIONS

- Biofilm discretization has a considerable impact on simulation results, especially when simulating mixed-culture biofilms having appreciable concentrations of different bacteria. Biofilm discretization (number of layers) should be chosen such that the biofilm model

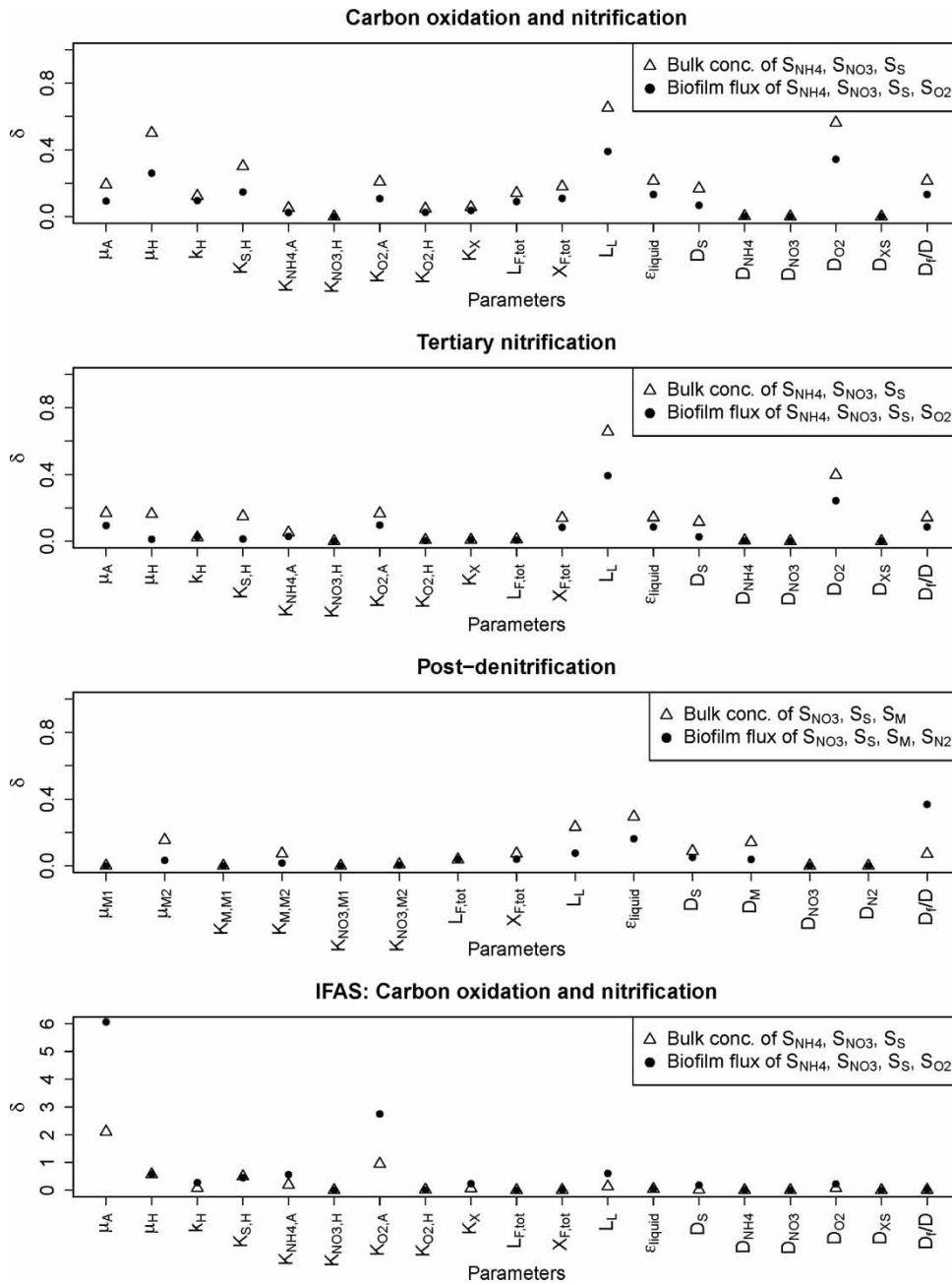


Figure 2 | Sensitivity measures δ for biokinetic and biofilm parameters for simulations at 12 °C (Scenario VI). For combined carbon oxidation and nitrification, tertiary nitrifications, and IFAS, δ is given for bulk concentrations of ammonium, nitrate and organic carbon (together), and fluxes of ammonium, nitrate, organic carbon, and oxygen (together). For tertiary denitrification, δ is given for bulk concentrations of nitrate, organic carbon, and methanol (together), and fluxes of nitrate, organic carbon, methanol, and di-nitrogen. Note that for IFAS, the scale of the y-axis is different.

appropriately reflects internal substrate and biomass gradients. A failure to properly discretize the biofilm may result in erroneous model results.

- Both benchmark simulations and sensitivity analyses have shown that model results are strongly influenced by the MTBL thickness (L_L). An accurate description of soluble

substrate concentration gradients external to the biofilm surface is critical to obtaining accurate simulation results from a biofilm (reactor) model. Additional research is needed to develop a protocol/procedure for the determination of the MTBL thickness for different biofilm reactor (and media) types and system configurations.

No simple recommendations for a generally applicable model calibration methodology can be suggested presently. However, sensitivity analyses have been demonstrated to be valuable, and can help with indentifying sensitive parameter subsets for biofilm model calibration. A local sensitivity analysis, however, should be carried out at different critical operating conditions (and potentially different locations within the wastewater treatment plant) as sensitivity of model predictions very much depends on environmental conditions (e.g. temperature) and treatment objectives (e.g. nitrification, denitrification).

REFERENCES

- Beyenal, H. & Lewandowski, Z. 2000 Combined effect of substrate concentration and flow velocity on effective diffusivity in biofilms. *Water Research* **34** (2), 528–538.
- Beyenal, H., Tanyolac, A. & Lewandowski, Z. 1998 Measurement of local effective diffusivity in heterogeneous biofilms. *Water Science and Technology* **38** (8–9), 171–178.
- Bilyk, K., Takács, I., Rohrbacher, J., Pitt, P., Latimer, R. & Dold, P. 2008 Full-scale testing advances fundamental understanding of denitrification filters. In *81st Annual Water Environment Federation Technical Exhibition and Conference (WEFTEC), October 18–22, 2008, Chicago (IL), USA*.
- Boltz, J. P. & Daigger, G. T. 2010 Uncertainty in bulk-liquid hydrodynamics and biofilm dynamics creates uncertainties in biofilm reactor design. *Water Science and Technology* **61** (2), 307–316.
- Boltz, J. P., Morgenroth, E., deBarbadillo, C., Dempsey, M., McQuarrie, J., Ghylis, T., Harrison, J. & Nerenberg, R. 2010a Biofilm reactor technology and design (Chapter 13). In: *Design of Municipal Wastewater Treatment Plants* (A. B. Pincince, ed.), Vol. 2, 5th edition, WEF Manual of Practice No. 8, ASCE Manuals and Reports on Engineering Practice No. 76, McGraw Hill, New York, USA.
- Boltz, J. P., Morgenroth, E. & Sen, D. 2010b Mathematical modelling of biofilms and biofilm reactors for engineering design. *Water Science & Technology* **62** (8), 1821–1836.
- Brockmann, D. & Morgenroth, E. 2007 Comparing global sensitivity analysis for a biofilm model for two-step nitrification using the qualitative screening method of Morris or the quantitative variance-based Fourier amplitude sensitivity test (FAST). *Water Science and Technology* **56** (8), 85–93.
- Brockmann, D., Rosenwinkel, K. H. & Morgenroth, E. 2007 Estimation of kinetic parameters of a model for deammonification in biofilms and evaluation of the model. *Water Science and Technology* **55** (8–9), 291–299.
- Brockmann, D., Rosenwinkel, K. H. & Morgenroth, E. 2008 Practical identifiability of biokinetic parameters of a model describing two-step nitrification in biofilms. *Biotechnology and Bioengineering* **101** (3), 497–514.
- Brun, R., Kühni, M., Siegrist, H., Gujer, W. & Reichert, P. 2002 Practical identifiability of ASM2d parameters – systematic selection and tuning of parameter subsets. *Water Research* **36** (16), 4113–4127.
- Brun, R., Reichert, P. & Kunsch, H. R. 2001 Practical identifiability analysis of large environmental simulation models. *Water Resources Research* **37** (4), 1015–1030.
- Eleiter, D., Milferstedt, K., Zhang, W., Hausner, M. & Morgenroth, E. 2007 Influence of detachment on substrate removal and microbial ecology in a heterotrophic/autotrophic biofilm. *Water Research* **41** (20), 4657–4671.
- Hauduc, H., Rieger, L., Ohtsuki, T., Shaw, A., Takács, I., Winkler, S., Héduit, A., Vanrolleghem, P. A. & Gillot, S. 2011 Activated sludge modelling: development and potential use of a practical applications database. *Water Science and Technology* **63** (10), 2164–2182.
- Henze, M., Gujer, W., Mino, T. & van Loosdrecht, M. 2000 *Activated Sludge Models ASM1, ASM2, ASM2d and ASM3*. IWA, London.
- Horn, H. & Hempel, D. C. 1995 Mass transfer coefficients for an autotrophic and a heterotrophic biofilm system. *Water Science and Technology* **32** (8), 199–204.
- Kim, H.-S., Pei, R., Boltz, J. P., Gellner, W. J., Gunsch, C., Freudenberg, R. G., Dodson, R. & Schuler, A. J. 2010 Attached and suspended phase nitrifying microbial community structures and functions in integrated fixed film activated sludge. *Water Environment Research* (in press).
- Kindaichi, T., Ito, T. & Okabe, S. 2004 Ecophysiological interaction between nitrifying bacteria and heterotrophic bacteria in autotrophic nitrifying biofilms as determined by microautoradiography-fluorescence in situ hybridization. *Applied and Environmental Microbiology* **70** (3), 1641–1650.
- Kissel, J. C., McCarty, P. L. & Street, R. L. 1984 Numerical-simulation of mixed-culture biofilm. *Journal of Environmental Engineering-ASCE* **110** (2), 393–411.
- Lewandowski, Z., Stoodley, P., Altobelli, S. & Fukushima, E. 1994 Hydrodynamics and kinetics in biofilm systems-recent advances and new problems. *Water Science and Technology* **29** (10–11), 223–229.
- McQuarrie, J. P. & Boltz, J. P. 2011 Moving bed biofilm reactor technology: process applications, design, and performance. *Water Environment Research* (in press).
- Morgenroth, E. 2003 Detachment-an often overlooked phenomenon in biofilm research and modelling. In: *Biofilms in Wastewater Treatment* (S. Wuertz, P. A. Wilderer & P. L. Bishop, eds.). IWA Publishing, London.
- Morgenroth, E., Eberl, H. J. & van Loosdrecht, M. C. M. 2000 Evaluating 3-D and 1-D mathematical models for mass transport in heterogeneous biofilms. *Water Science and Technology* **41** (4–5), 347–356.
- Morgenroth, E. & Wilderer, P. A. 2000 Influence of detachment mechanisms on competition in biofilms. *Water Research* **34** (2), 417–426.
- Okabe, S., Hirata, K. & Watanabe, Y. 1995 Dynamic changes in spatial microbial distribution in mixed-population biofilms:

- experimental results and model simulation. *Water Science and Technology* **32** (8), 67–74.
- Okabe, S., Naitoh, H., Satoh, H. & Watanabe, Y. 2002 Structure and function of nitrifying biofilms as determined by molecular techniques and the use of microelectrodes. *Water Science and Technology* **46** (1–2), 233–241.
- Okabe, S., Satoh, H. & Watanabe, Y. 1999 In situ analysis of nitrifying biofilms as determined by in situ hybridization and the use of microelectrodes. *Applied and Environmental Microbiology* **65** (7), 3182–3191.
- Reichert, P. 1998 AQUASIM 2.0-User Manual. Computer program for the identification and simulation of aquatic systems. Swiss Federal Institute for Environmental Science and Technology (EAWAG), Dübendorf, CH.
- Rittmann, B. & McCarty, P. L. 2001 *Environmental Biotechnology: Principles and Applications*, McGraw Hill.
- Rittmann, B. E. & Manem, J. A. 1992 Development and experimental evaluation of a steady-state, multispecies biofilm model. *Biotechnology and Bioengineering* **39** (9), 914–922.
- Schramm, A., Larsen, L. H., Revsbech, N. P., Ramsing, N. B., Amann, R. & Schleifer, K. H. 1996 Structure and function of a nitrifying biofilm as determined by in situ hybridization and the use of microelectrodes. *Applied and Environmental Microbiology* **62** (12), 4641–4647.
- Sin, G., Van Hulle, S. W. H., De Pauw, D. J. W., van Griensven, A. & Vanrolleghem, P. A. 2005 A critical comparison of systematic calibration protocols for activated sludge models: a SWOT analysis. *Water Research* **39** (12), 2459–2474.
- Sin, G., Weijma, J., Spanjers, H. & Nopens, I. 2008 Dynamic model development and validation for a nitrifying moving bed biofilter: effect of temperature and influent load on the performance. *Process Biochemistry* **43** (4), 384–397.
- Smets, B. F., Riefler, R. G., Lendenmann, U. & Spain, J. C. 1999 Kinetic analysis of simultaneous 2,4-dinitrotoluene (DNT) and 2,6-DNT biodegradation in an aerobic fluidized-bed biofilm reactor. *Biotechnology and Bioengineering* **63** (6), 642–653.
- Stewart, P. S. 1998 A review of experimental measurements of effective diffusive permeabilities and effective diffusion coefficients in biofilms. *Biotechnology and Bioengineering* **59** (3), 261–272.
- Van Hulle, S. W. H., Maertens, J., De Pauw, D. J. W. & Vanrolleghem, P. 2004 Using parameter sensitivity analysis of the CANON biofilm process: what to measure, where to measure and under which conditions? In: *Water and Environment Management Series: Young Researchers 2004* (P. Lens & R. M. Stuetz, eds.). IWA Publishing, London, UK, pp. 59–66.
- Wanner, O., Eberl, H., Morgenroth, E., Noguera, D., Picioreanu, C., Rittmann, B. & van Loosdrecht, M. C. M. 2006 *Mathematical Modeling of Biofilms*. IWA Publishing, London, UK.
- Wanner, O. & Gujer, W. 1984 Competition in biofilms. *Water Science and Technology* **17** (2–3), 27–44.
- Zhang, T. C. & Bishop, P. L. 1994a Density, porosity, and pore structure of biofilms. *Water Research* **28** (11), 2267–2277.
- Zhang, T. C. & Bishop, P. L. 1994b Evaluation of tortuosity factors and effective diffusivities in biofilms. *Water Research* **28** (11), 2279–2287.
- Zhang, T. C., Fu, Y. C. & Bishop, P. L. 1994 Competition in Biofilms. *Water Science and Technology* **29** (10–11), 263–270.
- Zhu, S. M. & Chen, S. L. 2001 Impacts of Reynolds number on nitrification biofilm kinetics. *Aquacultural Engineering* **24** (3), 213–229.

Systematic evaluation of biofilm models for engineering practice: components and critical assumptions

Supplementary material for 'Systematic evaluation of biofilm models for engineering practice: components and critical assumptions' by Boltz *et al.* (2011)

The following supplemental information is provided to describe (1) the model used for the study, (2) default parameter values, and (3) the parameter values and uncertainty ranges used for the local sensitivity analysis.

Temperature dependency of diffusion coefficients was accounted for according to:

$$D(T) = D(20^\circ\text{C}) \cdot \frac{273 + T}{273 + 20^\circ\text{C}} \cdot \frac{\mu(20^\circ\text{C})}{\mu(T)}$$

where D is the diffusion coefficient, T the temperature in $^\circ\text{C}$, and μ the dynamic viscosity of water in $\text{N m}^{-2} \text{s}$. The MTBL thickness, L_L , was estimated from fluid dynamics using a method similar to the one described by Morgenroth (2008):

$$L_L = \frac{L_c}{Sh}$$

where L_c is a characteristic length (which in this case is the flow-through radius of the biofilm carrier minus the biofilm thickness; the biofilm carrier flow through radius is 0.00455 m in Veolia AnoxKaldness Process K1 medium (Veolia, Paris, France) according to media parameters presented by Rusten *et al.* (2006), and Sh is the non-dimensional Sherwood number. The following empirical correlation was used to calculate the Sherwood number:

$$Sh = A + B \cdot Re^m \cdot Sc^n$$

The following empirical parameter values and relationships were applied to estimate L_L .

$A = 2.0$ (value by Rowe *et al.* (1965) for spherical particles)
 $B = 0.8$ (value by Rowe *et al.* (1965) for spherical particles)
 $m = 1/2$ (value by Rowe *et al.* (1965) for spherical particles)
 $n = 1/3$ (value by Rowe *et al.* (1965) for spherical particles)

$Re = \text{Reynolds number} = (U \cdot L_c)/\nu$

$U = \text{water velocity in vicinity of biofilm surface} \sim 5,000 \text{ m/d}$
 (after work presented by Boltz *et al.* 2009)

$\nu = \text{kinematic viscosity of water} = 1.0 \times 10^{-6} \text{ m}^2/\text{s}$

$Sc = \text{Schmidt number} = \nu/D_{W,i}$

$D_{W,i} = \text{diffusion coefficient of substance } i \text{ in water (m}^2/\text{d)}$

doi: 10.2166/wst.2011.709Supplement

X_{TSS} was calculated from the particulate state variables:

$$\begin{aligned} X_{TSS,bulk} &= X_{TSS,inorganic,in} + i_{TSBM} \cdot (X_{A,bulk} \\ &\quad + X_{H,bulk} + X_{M1,bulk} + X_{M2,bulk}) \\ &\quad + i_{TSXS} \cdot X_{S,bulk} + i_{TSXI} \cdot X_{I,bulk} \\ X_{TSS,biofilm} &= i_{TSBM} \cdot (X_{A,biofilm} \\ &\quad + X_{H,biofilm} + X_{M1,bulk} + X_{M2,bulk}) \\ &\quad + i_{TSXS} \cdot X_{S,biofilm} + i_{TSXI} \cdot X_{I,biofilm} \end{aligned}$$

where $X_{TSS,inorganic,in}$ is the amount of total suspended solids that is not accounted for by influent concentrations of X_S , X_H , X_A , X_{M1} , X_{M2} , and X_I .

Table S1 | State variables for the modified ASM3 without storage

Symbol	Description	Unit
<i>Dissolved components:</i>		
S_S	Readily biodegradable organic matter	g COD m^{-3}
S_I	Soluble inert organic matter	g COD m^{-3}
S_{N2}	Dinitrogen, N_2	g N m^{-3}
S_{NH4}	Ammonium	g N m^{-3}
S_{NO3}	Nitrate	g N m^{-3}
S_{O2}	Dissolved oxygen	g COD m^{-3}
S_{ALK}	Alkalinity	mole $\text{HCO}_3^- \text{ L}^{-1}$
S_M	Methanol	g COD m^{-3}
<i>Particulate components:</i>		
X_H	Heterotrophic organisms	g COD m^{-3}
X_I	Inert particulate organic matter	g COD m^{-3}
X_S	Slowly biodegradable organic organic matter	g COD m^{-3}
X_A	Nitrifying organisms	g COD m^{-3}
X_{TSS}^*	Total suspended solids	g COD m^{-3}
X_{M1}	Methanol degraders type 1	g COD m^{-3}
X_{M2}	Methanol degraders type 2	g COD m^{-3}

*Not introduced as state variable, but calculated from the state variables X_H , X_A , X_I , X_S , X_{M1} , and X_{M2} .

Table S2 | Stoichiometric parameter values for the modified ASM3 without storage used in the biofilm simulation benchmark. Unless otherwise noted, values are from Henze et al. (2000)

Symbol	Description	Value	Unit
Conversion factors			
<i>Nitrogen:</i>			
<i>Soluble Material</i>			
i_{NSI}	Nitrogen content of inert soluble COD, S_I	0.01	$g\ N\ g^{-1}\ COD$
i_{NSS}	Nitrogen content of readily biodegradable organic matter, S_S	0.03	$g\ N\ g^{-1}\ COD$
<i>Particulate Material</i>			
i_{NXI}	Nitrogen content of inert particulate COD, X_I	0.02	$g\ N\ g^{-1}\ COD$
i_{NXS}	Nitrogen content of slowly biodegradable organic matter, X_S	0.04	$g\ N\ g^{-1}\ COD$
i_{NBM}	Nitrogen content of biomass, X_H, X_A, X_{M1}, X_{M2}	0.07	$g\ N\ g^{-1}\ COD$
<i>Total Suspended Solids:</i>			
i_{TSSXI}	TSS to COD ratio for X_I	0.75	$g\ TSS\ g^{-1}\ COD$
i_{TSSXS}	TSS to COD ratio for X_S	0.75	$g\ TSS\ g^{-1}\ COD$
i_{TSSBM}	TSS to COD ratio for biomass, X_H, X_A, X_{M1}, X_{M2}	0.90	$g\ TSS\ g^{-1}\ COD$
Stoichiometric parameters			
<i>Hydrolysis</i>			
f_{SI}	Production of S_I in hydrolysis	0.1	$g\ COD\ g^{-1}\ COD$
<i>Heterotrophic biomass</i>			
$Y_{H,O2}$	Yield of heterotrophs using oxygen	0.63	$g\ COD\ g^{-1}\ COD$
$Y_{H,NO}$	Yield of heterotrophs using nitrate	0.54	$g\ COD\ g^{-1}\ COD$
f_{XI}	Production of X_I in endogenous respiration	0.2	$g\ COD\ g^{-1}\ COD$
<i>Autotrophic biomass</i>			
Y_A	Yield of autotrophs	0.24	$g\ COD\ g^{-1}\ COD$
f_{XI}	Production of X_I in endogenous respiration	0.2	$g\ COD\ g^{-1}\ COD$
<i>Methanol degraders type 1</i>			
Y_{M1}	Yield of methanol degraders type 1	0.58*	$g\ COD\ g^{-1}\ COD$
f_{XI}	Production of X_I in endogenous respiration	0.2	$g\ COD\ g^{-1}\ COD$
<i>Methanol degraders type 2</i>			
Y_{M2}	Yield of methanol degraders type 2	0.44*	$g\ COD\ g^{-1}\ COD$
f_{XI}	Production of X_I in endogenous respiration	0.2	$g\ COD\ g^{-1}\ COD$

*Boltz et al. (2009).

Table S3 | Kinetic parameter values (at 20 °C) for the modified ASM3 without storage used in the biofilm simulation benchmark. Unless otherwise noted, values are from Henze et al. (2000)

Symbol	Description	Value	Unit	θ
<i>Hydrolysis of particulate substrates: X_S</i>				
k_h	Hydrolysis rate constant	3.00	d^{-1}	1.041
K_X	Hydrolysis saturation constant	1.00	$g\ X_S\ g^{-1}\ X_H$	–
<i>Heterotrophic organisms: X_H</i>				
μ_H	Maximum growth rate on substrate	6.00	d^{-1}	1.072
$\eta_{NO3,H}$	Reduction factor for denitrification	0.80	–	–
$b_{H,O2}$	Aerobic endogenous respiration rate of X_H	0.20	d^{-1}	1.072

(continued)

Table S3 | continued

Symbol	Description	Value	Unit	θ
$b_{H,NO}$	Anoxic endogenous respiration rate of X_H	0.10	d^{-1}	1.072
$K_{O_2,H}$	Saturation/inhibition coefficient for oxygen	0.10*	$g\ O_2\ m^{-3}$	–
K_S	Saturation coefficient for growth on S_S	4.00*	$g\ COD\ m^{-3}$	–
$K_{NO_3,H}$	Saturation/inhibition coefficient for nitrate	0.14**	$g\ N\ m^{-3}$	–
$K_{NH_4,H}$	Saturation coefficient for ammonium (nutrient)	0.01	$g\ N\ m^{-3}$	–
$K_{ALK,H}$	Saturation coefficient for alkalinity (HCO_3^-)	0.10	$mole\ HCO_3^-\ m^{-3}$	–
<i>Nitrifying (autotrophic) organisms: X_A</i>				
μ_A	Maximum growth rate of X_A	1.00	d^{-1}	1.111
b_{A,O_2}	Aerobic endogenous respiration rate of X_A	0.15	d^{-1}	1.116
$b_{A,NO}$	Anoxic endogenous respiration rate of X_A	0.05	d^{-1}	1.116
$K_{O_2,A}$	Saturation coefficient for oxygen	0.80*	$g\ O_2\ m^{-3}$	–
$K_{NH_4,A}$	Saturation coefficient for ammonium (substrate)	0.70**	$g\ N\ m^{-3}$	–
$K_{NO_3,A}$	Saturation/inhibition coefficient for nitrate	0.14***	$g\ N\ m^{-3}$	–
$K_{ALK,A}$	Saturation coefficient for alkalinity (HCO_3^-)	0.40*	$mole\ HCO_3^-\ m^{-3}$	–
<i>Methanol degraders type 1: X_{M1}****</i>				
μ_{M1}	Maximum growth rate on substrate	2.56	d^{-1}	1.13
$\eta_{NO_3,M1}$	Reduction factor for denitrification	0.20	–	–
b_{M1}	Endogenous respiration rate of X_{M1}	0.03	d^{-1}	1.029
$K_{O_2,M1}$	Saturation/inhibition coefficient for oxygen	0.50	$g\ O_2\ m^{-3}$	–
$K_{M,M1}$	Saturation coefficient for growth on S_S	0.50	$g\ COD\ m^{-3}$	–
$K_{NO_3,M1}$	Saturation/inhibition coefficient for nitrate	0.80	$g\ N\ m^{-3}$	–
$K_{NH_4,M1}$	Saturation coefficient for ammonium (nutrient)	0.005	$g\ N\ m^{-3}$	–
$K_{ALK,M1}$	Saturation coefficient for alkalinity (HCO_3^-)	0.10	$mole\ HCO_3^-\ m^{-3}$	–
<i>Methanol degraders type 2: X_{M2}****</i>				
μ_{M2}	Maximum growth rate on substrate	1.28	d^{-1}	1.13
$\eta_{NO_3,M2}$	Reduction factor for denitrification	1.00	–	–
b_{M2}	Endogenous respiration rate of X_{M1}	0.03	d^{-1}	1.029
$K_{O_2,M2}$	Saturation/inhibition coefficient for oxygen	0.50	$g\ O_2\ m^{-3}$	–
$K_{M,M2}$	Saturation coefficient for growth on S_S	0.50	$g\ COD\ m^{-3}$	–
$K_{NO_3,M2}$	Saturation/inhibition coefficient for nitrate	0.10	$g\ N\ m^{-3}$	–
$K_{NH_4,M2}$	Saturation coefficient for ammonium (nutrient)	0.005	$g\ N\ m^{-3}$	–
$K_{ALK,M2}$	Saturation coefficient for alkalinity (HCO_3^-)	0.10	$mole\ HCO_3^-\ m^{-3}$	–

*this study, **Wiesmann (1994), ***set to the same value as $K_{NO_3,H}$, ****Boltz et al. (2009).

Table S4 | Biofilm parameters and diffusion coefficients

Symbol	Description	Value	Unit
<i>Diffusion coefficients in water</i>			
D_S	Readily biodegradable organic matter	1.0×10^{-4}	$m^2\ d^{-1}$
D_{O_2}	Oxygen	2.1×10^{-4}	$m^2\ d^{-1}$
D_{NH_4}	Ammonium	1.7×10^{-4}	$m^2\ d^{-1}$

(continued)

Table S4 | continued

Symbol	Description	Value	Unit
D_{NO_3}	Nitrate	1.6×10^{-4}	$m^2 d^{-1}$
D_{N_2}	Dinitrogen	2.1×10^{-4}	$m^2 d^{-1}$
D_{ALK}	Alkalinity	1.0×10^{-4}	$m^2 d^{-1}$
D_{SI}	Soluble inerts	1.0×10^{-4}	$m^2 d^{-1}$
D_{XS}	Slowly biodegradable organic matter	$0.6 \times 10^{-4} (*)$	$m^2 d^{-1}$
D_M	Methanol (only denitrification system)	1.5×10^{-4}	$m^2 d^{-1}$
<i>Biofilm parameters</i>			
D_F/D	Ratio of diffusion in biofilm to diffusion in water	0.8	–
ϵ_l	Fraction of the liquid volume in the biofilm	0.8	–
$X_{F,tot}$	Biofilm density	25,000	$g\ COD_X/m^3$
ρ_X	Biomass density in the biofilm ($X_{F,tot}/(1-\epsilon_l)$)	125,000	$g\ COD_X/m^3$
$L_{F,tot}$	Biofilm thickness	200	μm
L_L	External mass transfer layer thickness	100	μm

*The value for the diffusion coefficient for slowly biodegradable substrate may vary considerably.

Table S5 | Process rate equations for the modified ASM3 without storage as used in the biofilm simulation benchmark (Henze et al. 2000)

Process	Process rate equation
<i>Hydrolysis processes:</i>	
1 Aerobic hydrolysis	$k_H \cdot \frac{X_S/X_H}{K_X+X_S/X_H} \cdot X_H$
<i>Heterotrophic organisms: X_H</i>	
2 Aerobic growth of X_H	$\mu_H \cdot \frac{S_{O_2}}{K_{O_2,H}+S_{O_2}} \cdot \frac{S_S}{K_S+S_S} \cdot \frac{S_{NH_4}}{K_{NH_4,H}+S_{NH_4}} \cdot \frac{S_{ALK}}{K_{ALK,H}+S_{ALK}} \cdot X_H$
3 Anoxic growth of X_H	$\mu_H \cdot \eta_{NO_3,H} \cdot \frac{K_{O_2,H}}{K_{O_2,H}+S_{O_2}} \cdot \frac{S_{NO_3}}{K_{NO_3,H}+S_{NO_3}} \cdot \frac{S_S}{K_S+S_S} \cdot \frac{S_{NH_4}}{K_{NH_4,H}+S_{NH_4}} \cdot \frac{S_{ALK}}{K_{ALK,H}+S_{ALK}} \cdot X_H$
4 Aerobic endogenous respiration of X_H	$b_{H,O_2} \cdot \frac{S_{O_2}}{K_{O_2,H}+S_{O_2}} \cdot X_H$
5 Anoxic endogenous respiration of X_H	$b_{H,NO} \cdot \frac{K_{O_2,H}}{K_{O_2,H}+S_{O_2}} \cdot \frac{S_{NO_3}}{K_{NO_3,H}+S_{NO_3}} \cdot X_H$
<i>Nitrifying organisms: X_A</i>	
6 Aerobic growth of X_A	$\mu_A \cdot \frac{S_{O_2}}{K_{O_2,A}+S_{O_2}} \cdot \frac{S_{NH_4}}{K_{NH_4,A}+S_{NH_4}} \cdot \frac{S_{ALK}}{K_{ALK,A}+S_{ALK}} \cdot X_A$
7 Aerobic endogenous respiration of X_A	$b_{A,O_2} \cdot \frac{S_{O_2}}{K_{O_2,A}+S_{O_2}} \cdot X_A$
8 Anoxic endogenous respiration of X_A	$b_{A,NO} \cdot \frac{K_{O_2,H}}{K_{O_2,A}+S_{O_2}} \cdot \frac{S_{NO_3}}{K_{NO_3,A}+S_{NO_3}} \cdot X_A$
<i>Methylootrophs 1: X_{M1}</i>	
9 Aerobic growth of X_{M1}	$\mu_{M1} \cdot \frac{S_{O_2}}{K_{O_2,M1}+S_{O_2}} \cdot \frac{S_M}{K_{M1}+S_M} \cdot \frac{S_{NH_4}}{K_{NH_4,M1}+S_{NH_4}} \cdot \frac{S_{ALK}}{K_{ALK,M1}+S_{ALK}} \cdot X_{M1}$
10 Anoxic growth of X_{M1}	$\mu_{M1} \cdot \eta_{NO_3,M1} \cdot \frac{K_{O_2,M1}}{K_{O_2,M1}+S_{O_2}} \cdot \frac{S_{NO_3}}{K_{NO_3,M1}+S_{NO_3}} \cdot \frac{S_M}{K_{M1}+S_M} \cdot \frac{S_{NH_4}}{K_{NH_4,M1}+S_{NH_4}} \cdot \frac{S_{ALK}}{K_{ALK,M1}+S_{ALK}} \cdot X_{M1}$
11 Aerobic endogenous respiration of X_{M1}	$b_{M1} \cdot \frac{S_{O_2}}{K_{O_2,M1}+S_{O_2}} \cdot X_{M1}$
12 Anoxic endogenous respiration of X_{M1}	$b_{M1} \cdot \frac{K_{O_2,M1}}{K_{O_2,M1}+S_{O_2}} \cdot \frac{S_{NO_3}}{K_{NO_3,M1}+S_{NO_3}} \cdot X_{M1}$
<i>Methylootrophs 2: X_{M2}</i>	
13 Aerobic growth of X_{M2}	$\mu_{M2} \cdot \frac{S_{O_2}}{K_{O_2,M2}+S_{O_2}} \cdot \frac{S_M}{K_{M2}+S_M} \cdot \frac{S_{NH_4}}{K_{NH_4,M2}+S_{NH_4}} \cdot \frac{S_{ALK}}{K_{ALK,M2}+S_{ALK}} \cdot X_{M2}$
14 Anoxic growth of X_{M2}	$\mu_{M2} \cdot \eta_{NO_3,M2} \cdot \frac{K_{O_2,M2}}{K_{O_2,M2}+S_{O_2}} \cdot \frac{S_{NO_3}}{K_{NO_3,M2}+S_{NO_3}} \cdot \frac{S_M}{K_{M2}+S_M} \cdot \frac{S_{NH_4}}{K_{NH_4,M2}+S_{NH_4}} \cdot \frac{S_{ALK}}{K_{ALK,M2}+S_{ALK}} \cdot X_{M2}$
15 Aerobic endogenous respiration of X_{M2}	$b_{M2} \cdot \frac{S_{O_2}}{K_{O_2,M2}+S_{O_2}} \cdot X_{M2}$
16 Anoxic endogenous respiration of X_{M2}	$b_{M2} \cdot \frac{K_{O_2,M2}}{K_{O_2,M2}+S_{O_2}} \cdot \frac{S_{NO_3}}{K_{NO_3,M2}+S_{NO_3}} \cdot X_{M2}$

Table S6 | Stoichiometric matrix of soluble state variables for the modified ASM3 without storage as used in the biofilm simulation benchmark (Henze et al. 2000; Boltz et al. 2009)

Process	S _{O2}	S _S	S _I	S _{NH4}	S _{NO3}	S _{N2}	S _{ALK}	S _M
<i>Hydrolysis processes:</i>								
1 Aerobic hydrolysis		1-f _{SI}	f _{SI}	v _{1,NH4}			v _{1,ALK}	
<i>Heterotrophic organisms: X_H</i>								
2 Aerobic growth of X _H	-(1-Y _{H,O2})/Y _{H,O2}	-1/Y _{H,O2}		v _{2,NH4}			v _{2,ALK}	
3 Anoxic growth of X _H		-1/Y _{H,NO}		v _{3,NH4}	-(1-Y _{H,NO})/(2.86 · Y _{H,NO})	(1-Y _{H,NO})/(2.86 · Y _{H,NO})	v _{3,ALK}	
4 Aerobic endogenous respiration of X _H	-(1-f _{XI})			v _{4,NH4}			v _{4,ALK}	
5 Anoxic endogenous respiration of X _H				v _{5,NH4}	-(1-f _{XI})/2.86	(1-f _{XI})/2.86	v _{5,ALK}	
<i>Nitrifying organisms: X_A</i>								
6 Aerobic growth of X _A	-(4.57-Y _A)/Y _A			v _{6,NH4}	1/Y _A		v _{6,ALK}	
7 Aerobic endogenous respiration of X _A	-(1-f _{XI})			v _{7,NH4}			v _{7,ALK}	
8 Anoxic endogenous respiration of X _A				v _{8,NH4}	-(1-f _{XI})/2.86	(1-f _{XI})/2.86	v _{8,ALK}	
<i>Methylotrophs 1: X_{M1}</i>								
9 Aerobic growth of X _{M1}	-(1-Y _{M1})/Y _{M1}			v _{9,NH4}			v _{9,ALK}	-1/Y _{M1}
10 Anoxic growth of X _{M1}				v _{10,NH4}	-(1-Y _{M1})/(2.86 · Y _{M1})	(1-Y _{M1})/(2.86 · Y _{M1})	v _{10,ALK}	-1/Y _{M1}
11 Aerobic endogenous respiration of X _{M1}	-(1-f _{XI})			v _{11,NH4}			v _{11,ALK}	
12 Anoxic endogenous respiration of X _{M1}				v _{12,NH4}	-(1-f _{XI})/2.86	(1-f _{XI})/2.86	v _{12,ALK}	
<i>Methylotrophs 2: X_{M2}</i>								
13 Aerobic growth of X _{M2}	-(1-Y _{M2})/Y _{M2}			v _{13,NH4}			v _{13,ALK}	-1/Y _{M2}
14 Anoxic growth of X _{M2}				v _{14,NH4}	-(1-Y _{M2})/(2.86 · Y _{M2})	(1-Y _{M2})/(2.86 · Y _{M2})	v _{14,ALK}	-1/Y _{M2}
15 Aerobic endogenous respiration of X _{M2}	-(1-f _{XI})			v _{15,NH4}			v _{15,ALK}	
16 Anoxic endogenous respiration of X _{M2}				v _{16,NH4}	-(1-f _{XI})/2.86	(1-f _{XI})/2.86	v _{16,ALK}	

Table S7 | Stoichiometric matrix of particulate state variables for the modified ASM3 without storage as used in the biofilm simulation benchmark (Henze et al. 2000; Boltz et al. 2009)

Process	X _S	X _H	X _A	X _I	X _{M1}	X _{M2}
<i>Hydrolysis processes:</i>						
1 Aerobic hydrolysis	-1					
<i>Heterotrophic organisms: X_H</i>						
2 Aerobic growth of X _H		1				
3 Anoxic growth of X _H		1				
4 Aerobic endogenous respiration of X _H		-1		f _{XI}		
5 Anoxic endogenous respiration of X _H		-1		f _{XI}		

(continued)

Table S7 | continued

Process	X_S	X_H	X_A	X_I	X_{M1}	X_{M2}
<i>Nitrifying organisms: X_A</i>						
6 Aerobic growth of X_A			1			
7 Aerobic endogenous respiration of X_A			-1	f_{XI}		
8 Anoxic endogenous respiration of X_A			-1	f_{XI}		
<i>Methylootrophs 1: X_{M1}</i>						
9 Aerobic growth of X_{M1}					1	
10 Anoxic growth of X_{M1}					1	
11 Aerobic endogenous respiration of X_{M1}				f_{XI}	-1	
12 Anoxic endogenous respiration of X_{M1}				f_{XI}	-1	
<i>Methylootrophs 2: X_{M2}</i>						
13 Aerobic growth of X_{M2}						1
14 Anoxic growth of X_{M2}						1
15 Aerobic endogenous respiration of X_{M2}				f_{XI}		-1
16 Anoxic endogenous respiration of X_{M2}				f_{XI}		-1

Table S8 | Stoichiometric coefficients for S_{NH4} and S_{ALK}

Process	S_{NH4}	S_{ALK}
<i>Hydrolysis processes:</i>		
1 Aerobic hydrolysis	$v_{1,NH4} = i_{N,XS} - (1 - f_{SI}) \cdot i_{N,SS} - f_{SI} \cdot i_{N,SI}$	$v_{1,ALK} = (i_{N,XS} - (1 - f_{SI}) \cdot i_{N,SS} - f_{SI} \cdot i_{N,SI})/14$
<i>Heterotrophic organisms: X_H</i>		
2 Aerobic growth of X_H	$v_{2,NH4} = -i_{N,BM}$	$v_{2,ALK} = -i_{N,BM}/14$
3 Anoxic growth of X_H	$v_{3,NH4} = -i_{N,BM}$	$v_{3,ALK} = (-i_{N,BM} + (1 - Y_{H,NO})/(2.86 \cdot Y_{H,NO}))/14$
4 Aerobic endogenous respiration of X_H	$v_{4,NH4} = i_{N,BM} - f_{XI} \cdot i_{N,XI}$	$v_{4,ALK} = (i_{N,BM} - f_{XI} \cdot i_{N,XI})/14$
5 Anoxic endogenous respiration of X_H	$v_{5,NH4} = i_{N,BM} - f_{XI} \cdot i_{N,XI}$	$v_{5,ALK} = (i_{N,BM} - f_{XI} \cdot i_{N,XI} + (1 - f_{XI})/2.86)/14$
<i>Nitrifying organisms: X_A</i>		
6 Aerobic growth of X_A	$v_{6,NH4} = -1/Y_A - i_{N,BM}$	$v_{6,ALK} = (-1/Y_A - i_{N,BM} - 1/Y_A)/14$
7 Aerobic endogenous respiration of X_A	$v_{7,NH4} = i_{N,BM} - f_{XI} \cdot i_{N,XI}$	$v_{7,ALK} = (i_{N,BM} - f_{XI} \cdot i_{N,XI})/14$
8 Anoxic endogenous respiration of X_A	$v_{8,NH4} = i_{N,BM} - f_{XI} \cdot i_{N,XI}$	$v_{8,ALK} = (i_{N,BM} - f_{XI} \cdot i_{N,XI} + (1 - f_{XI})/2.86)/14$
<i>Methylootrophs type 1: X_{M1}</i>		
9 Aerobic growth of X_{M1}	$v_{9,NH4} = -i_{N,BM}$	$v_{9,ALK} = -i_{N,BM}/14$
10 Anoxic growth of X_{M1}	$v_{10,NH4} = -i_{N,BM}$	$v_{10,ALK} = (-i_{N,BM} + (1 - Y_{M1})/(2.86 \cdot Y_{M1}))/14$
11 Aerobic endogenous respiration of X_{M1}	$v_{11,NH4} = i_{N,BM} - f_{XI} \cdot i_{N,XI}$	$v_{11,ALK} = (i_{N,BM} - f_{XI} \cdot i_{N,XI})/14$
12 Anoxic endogenous respiration of X_{M1}	$v_{12,NH4} = i_{N,BM} - f_{XI} \cdot i_{N,XI}$	$v_{12,ALK} = (i_{N,BM} - f_{XI} \cdot i_{N,XI} + (1 - f_{XI})/2.86)/14$
<i>Methylootrophs type 2: X_{M2}</i>		
13 Aerobic growth of X_{M2}	$v_{13,NH4} = -i_{N,BM}$	$v_{13,ALK} = -i_{N,BM}/14$
14 Anoxic growth of X_{M2}	$v_{14,NH4} = -i_{N,BM}$	$v_{14,ALK} = (-i_{N,BM} + (1 - Y_{M1})/(2.86 \cdot Y_{M1}))/14$
15 Aerobic endogenous respiration of X_{M2}	$v_{15,NH4} = i_{N,BM} - f_{XI} \cdot i_{N,XI}$	$v_{15,ALK} = (i_{N,BM} - f_{XI} \cdot i_{N,XI})/14$
16 Anoxic endogenous respiration of X_{M2}	$v_{16,NH4} = i_{N,BM} - f_{XI} \cdot i_{N,XI}$	$v_{16,ALK} = (i_{N,BM} - f_{XI} \cdot i_{N,XI} + (1 - f_{XI})/2.86)/14$

Table S9 | Parameter values and uncertainty ranges used for local sensitivity analysis. The concept of defining uncertainty classes for biokinetic parameters was based on Brun et al. (2002)

Parameter	Unit	Value	Uncertainty range	Uncertainty class
μ_A	d^{-1}	1	0.2	2
μ_H	d^{-1}	6	3	3
μ_{M1}	d^{-1}	2.56	1.28	3
μ_{M2}	d^{-1}	1.28	0.64	3
k_H	d^{-1}	3	1.5	3
$K_{S,H}$	$g\ COD\ m^{-3}$	4	2	3
K_{M1}	$g\ COD\ m^{-3}$	0.5	0.25	3
K_{M2}	$g\ COD\ m^{-3}$	0.5	0.25	3
$K_{NH_4,A}$	$g\ N\ m^{-3}$	0.7	0.35	3
$K_{NO_3,H}$	$g\ N\ m^{-3}$	0.14	0.028	2
$K_{NO_3,M1}$	$g\ N\ m^{-3}$	0.8	0.4	3
$K_{NO_3,M2}$	$g\ N\ m^{-3}$	0.1	0.05	3
$K_{O_2,A}$	$g\ O_2\ m^{-3}$	0.8	0.4	3
$K_{O_2,H}$	$g\ O_2\ m^{-3}$	0.1	0.05	3
K_X	$g\ X_S\ g^{-1}\ X_H$	1	0.5	3
$L_{F,tot}$	μm	200	100	3
$X_{F,tot}$	$g\ COD_X/m^3$	25,000	5,000	2
L_L	μm	100	50	3
ϵ_{liquid}	-	0.8	0.16	2
D_S	$m^2\ d^{-1}$	1.0×10^{-4}	0.2×10^{-4}	2
D_{NH_4}	$m^2\ d^{-1}$	1.7×10^{-4}	0.34×10^{-4}	2
D_{NO_3}	$m^2\ d^{-1}$	1.6×10^{-4}	0.32×10^{-4}	2
D_{O_2}	$m^2\ d^{-1}$	2.1×10^{-4}	0.42×10^{-4}	2
D_{X_S}	$m^2\ d^{-1}$	0.6×10^{-4}	0.12×10^{-4}	2
D_{ALK}	$m^2\ d^{-1}$	1.0×10^{-4}	0.2×10^{-4}	2
D_{N_2}	$m^2\ d^{-1}$	2.1×10^{-4}	0.42×10^{-4}	2
D_M	$m^2\ d^{-1}$	1.5×10^{-4}	0.3×10^{-4}	2
D_f/D	-	0.8	0.16	2

REFERENCES

- Boltz, J. P., Johnson, B. R., Daigger, G. T. & Sandino, J. 2009 Modeling integrated fixed-film activated sludge and moving-bed biofilm reactor systems I: mathematical treatment and model Development. *Water Environment Research* **81**, 555–575.
- Boltz, J. P., E., Morgenroth, E., Brockmann, D., Bott, C., Gellner, W. J. & Vanrolleghem, P. A. 2011 Systematic evaluation of biofilm models for engineering practice: components and critical assumptions. *Water Science and Technology* **64**, 930–944.
- Brun, R., Kühni, M., Siegrist, H., Gujer, W. & Reichert, P. 2002 Practical identifiability of ASM2d parameters - systematic selection and tuning of parameter subsets. *Water Research* **36** (16), 4113–4127.
- Henze, M., Gujer, W., Mino, T. & van Loosdrecht, M. 2000 *Activated sludge models ASM1, ASM2, ASM2d and ASM3*, IWA, London.
- Morgenroth, E. 2008 Modelling biofilms. In: *Biological Wastewater Treatment - Principles, Modelling, and Design*. (M. Henze, M. C. M. van Loosdrecht & G. Ekama & D. Brdjanovic, eds.). IWA Publishing, London, UK.
- Rowe, P. N., Claxton, K. T. & Lewis, J. B. 1965 Heat and mass transfer from a single sphere in an extensive flowing fluid. *Transactions of the Institution of Chemical Engineers and the Chemical Engineer* **43**, 14–31.
- Rusten, B., Eikebrokk, B., Ulgenes, Y. & Lygren, E. 2006 Design and operations of the Kaldnes moving bed biofilm reactors. *Aquacultural Engineering* **34** (3), 322–331.
- Wiesmann, U. 1994 Biological nitrogen removal from wastewater. In: *Advances in Biochemical Engineering/Biotechnology*. Springer Berlin, Heidelberg, pp. 113–154.